COMPARISON OF FLUORESCENT PROTEIN LABELLED AND WILD TYPE NMDA RECEPTOR DISTRIBUTION

A THESIS SUBMITTED TO
THE GRADUATE SCHOOL OF NATURAL AND APPLIED SCIENCES OF
MIDDLE EAST TECHNICAL UNIVERSITY

BY

ŞERİFE ŞEYDA PİRİNÇCİ

IN PARTIAL FULFILLMENT OF THE REQUIREMENTS FOR
THE DEGREE OF MASTER OF SCIENCE IN
BIOLOGY

JANUARY 2013

Approval of the Thesis

COMPARISON OF FLUORESCENT PROTEIN LABELLED AND WILD TYPE NMDA RECEPTOR DISTRIBUTION

Submitted by **ŞERİFE ŞEYDA PİRİNÇCİ** in partial fulfillment of the requirement for the degree of **Master of Science in Biology Department**, **Middle East Technical University** by,

Prof. Dr. Canan Özgen
Dean, Graduate School of **Natural and Applied Sciences** _____

Prof. Dr. Gülay Özcengiz
Head of the Department, **Biology** _____

Assoc. Prof. Dr. Çağdaş D. Son
Supervisor, **Biology Dept., METU** _____

Examining Committee Members

Prof. Dr. Mahinur Akkaya
Chemistry Dept., METU _____

Assoc. Prof. Dr. Çağdaş D. Son
Biology Dept., METU _____

Assist. Prof. Dr. Tülin Yanık
Biology Dept., METU _____

Assist. Prof. Dr. Michelle Adams
Psychology Dept., Bilkent University _____

Assist. Prof. Dr. Hakan Kayır
Medical Pharmacology Dept., GATA _____

Date: 28.01.2013

I hereby declare that all information in this document has been obtained and presented in accordance with academic rules and ethical conduct. I also declare that, as required by these rules and conduct, I have fully cited and referenced all material and results that are not original to this work.

Name, Last name : Ş. Şeyda PİRİNÇCİ

Signature :

ABSTRACT

COMPARISON OF FLUORESCENT PROTEIN LABELLED AND WILD TYPE NMDA RECEPTOR DISTRIBUTION

Pirinçci, Şerife Şeyda
M.Sc., Department of Biology
Supervisor: Assoc. Prof. Dr. Çağdaş D. Son
January 2013, 63 pages

NMDA (N-methyl D-aspartate) Receptor is a ligand and voltage gated ion channel and involved in many processes such as synaptic plasticity, memory formation, behavioral responses and cell survival. In the sense of functional activity, cellular localization of NMDAR is important since this receptor shows its activity on the membrane. Although NMDA receptor is intensely studied there are no satisfying study showing its localization with microscobic methods. Besides, the effect of florescent protein labelling of NMDA receptor on its distribution is not shown. It is expected to provide basis for further interaction and distribution studies with this comparison.

Contrary to literature, in this study it is shown that NMDA receptor does not localize only in ER and membrane instead has a cytosolic pattern and this pattern is compatible with the distribution of wild type NMDA receptor. In addition, florescent protein labelling of NMDA receptor does not interrupt cellular distribution of NMDAR. Moreover, this study shows that N-terminal domain of NR1 subunit is sufficient to prevent degradation of NR2B in the cell.

In consideration of this study it can be concluded that EGFP and mCherry labelled NMDA receptors can be used in interaction studies such as FRET and other studies, making use of fluorescent labelling of NMDA receptors, in terms of cellular distribution.

Keywords: NMDA receptor, EGFP, mCherry, localization, distibution

ÖZ

DOĞAL VE FLORESAN PROTEİNLE İŞARETLENMİŞ NMDA RESEPTÖRLERİNİN HÜCRE İÇİNDE DAĞILIMININ KARŞILAŞTIRILMASI

Pirinçci, Şerife Şeyda
Yüksek Lisans, Biyoloji Bölümü
Tez Yöneticisi: Doç. Dr. Çağdaş D. Son
Ocak 2013, 63 sayfa

Bir ligand ve voltaj kapılı iyon kanalı olan NMDA (N-methyl D-aspartate) Reseptörü sinaptik plastisite, hafıza oluşumu, davranış yanıtı ve hücre hayatta kalması gibi önemli süreçlerde yer alır. NMDA Reseptörünün fonksiyonlarını gerçekleştirmesi açısından reseptörün hücre içerisinde bulunduğu yer önemlidir. Bu reseptör hücre zarında etkinlik gösterebilmektedir. Bugüne kadar NMDA reseptörü çokça çalışılmış olmasına karşın lokalizasyonunu mikroskobik yöntemlerle gösteren tatmin edici bir çalışma bulunmamaktadır.

Ayrıca, lokalizasyon ve reseptör etkileşimleri çalışmalarında önemli yer tuttuğu bilinen floresan proteinlerle işaretleme çalışmalarının NMDA reseptörünün dağılımını etkileyip etkilemediğini gösteren bir çalışma da bulunmamaktadır. Bu karşılaştırmanın yapılmasının ileride yapılacak olan etkileşim ve dağılım çalışmaları için temel oluşturması beklenmektedir.

Bu çalışmada literatürde belirtildiğinin aksine NMDA reseptörünün sadece ER ve hücre zarında lokalize olmadığı, daha çok sitozolik bir dağılım gösterdiği, bu sonucun doğal fare NMDA reseptörü ile örtüştüğü ve en azından dağılım açısından floresan proteinler ile işaretlemenin NMDA reseptörünün hücre içi dağılımını etkilemediği gösterilmiştir. Ayrıca NMDA reseptörünün alt birimlerinden biri olan NR2B altbiriminin hücrede varlığını sürdürebilmesi için NR1 altbiriminin N-terminal kısmının yeterli olduğu görülmüştür.

Bu çalışmanın ışığında, EGFP ve mCherry floresan proteinleri ile işaretlenen NMDA reseptörlerinin FRET metodu gibi NMDA reseptörlerinin etkileşimlerini gösterecek olan çalışmalarda kullanılmasında reseptör dağılımı açısından bir sakınca olmadığı söylenebilir.

Anahtar Kelimeler: NMDA reseptörü, EGFP, mCherry, lokalizasyon, dağılım

ACKNOWLEDGEMENT

First and foremost, I would like to thank my supervisor Assoc. Prof. Dr. Çağdaş D. SON for his valuable assistance, patience, support and guidance. This thesis study would not be completed without his support.

Deepest gratitude are also due to members of thesis examining committee; Prof. Dr. Mahinur AKKAYA, Assist. Prof. Dr. Tülin YANIK, Assist. Prof.. Dr. Hakan KAYIR and Assist. Prof. Dr. Michelle ADAMS without whose knowledge and guidance this study would not have been successful.

I also thank former and current members of SON's Lab ; Gökhan ÜNLÜ, Gözde KUMAŞ, Giray BULUT, Sinem ÇELEBİÖVEN, Beren ÜSTÜNKAYA, Orkun CEVHEROĞLU, Selin AKKUZU and of course İlke SÜDER for their endless support. I wouldn't complete this thesis without their help.

I would like to express my gratitude for my family Filiz PİRİNÇCİ, Hayrettin PİRİNÇCİ, Müberra GENÇ and Buğra GENÇ for their unequivocal understanding, encouragement and endless patience throughout my life. I also would like to thank Baby GENÇ for cheer and hope he brought our life.

I would like to thank UNAM for allowing us to use Confocal Microscopy Facilitiy.

In addition I would like to thank TUBITAK BIDEB-2210 Domestic Master Scholarship for their financial support throughout my graduate studies and IRG Marie Curie Actions for supporting this project.

Last but not the least; I would like to thank Uğur ÇETİN for his invaluable assistance, understanding, support and motivation. It would be impossible to write this thesis without him.

TABLE OF CONTENTS

LIST OF TABLES

TABLES

LIST OF FIGURES

FIGURES

LIST OF ABBREVIATIONS

ABD: Agonist binding domain
AMPA: α-amino-3-hydroxy-5-methyl-4-isoxazolepropionic acid
AMPAR: α-amino-3-hydroxy-5-methyl-4-isoxazolepropionic acid receptor
AP2: Adaptor protein 2
Bp: base pair
BSA: Bovine serum albumin
$CaCl_2$: Calcium chloride
CaMKII: Ca^{2+}/calmodulin-dependent protein kinase II
cDNA: Complementary Deoxyribonucleic acid
COPII: Coat protein II
CREB: cAMP response element-binding protein
CTD: C-terminal domain
D: Aspartic acid
DMEM: Dulbecco's modified eagle medium
DNA: Deoxyribonucleic acid
dNTP: Deoxyribonucleotide triphosphate
E.coli: Escherichia coli
E: Glutamic acid
EGFP: Enhanced Green Fluorescent Protein
ER: Endoplasmic reticulum
ERK: Extracellular signal regulated kinase
EtBr: Ethidium bromide
F: Phenylalanine
FACS: Fluorescence-activated cell sorting
FBS: Fetal bovine serum
FRET: Förster Resonance Energy Transfer
Glu: Glutamine
GluR: Glutamate Receptor
GPCR: G Protein Coupled Receptor
H: Histidine
ICC: Immunocytochemistry
KA: Kainate
KIF: Kinesin superfamily
L: Leucine
LB: Luria broth
LIVBP: Leucine/isoleucine/valine- binding protein
LTD: Long term depression
LTP: Long term potentiation

N2a: Neuro 2a
NMDA: N-methyl D- aspartate
NMDAR: N-methyl D-aspartate receptor
NTD: N-terminal domain
PBS: Phosphate Buffered Saline
PCR: Polymerase Chain Reaction
PCR: Polymerase chain reaction
PSD: Post synaptic density
QBP: Glutamine binding protein
R: Arginin
S:Serine
T:Threonine
Taq: Thermus aquaticus
TBE: Tris/Borate/EDTA
Tfb: Transformation buffer
TM: Transmembrane
TMD: Transmembrane domain
V: Valine
Y: Tyrosine

CHAPTER I

INTRODUCTION

1.1. ION CHANNELS

Ion channels are membrane proteins that provide rapid flow of ions to inward and outward of the cell. They are generally composed of more than one subunit and combination of these subunits form a central pore to let the passage of ions. By the use of ion channels several signalling pathways, electrical activity of neurons, membrane potential and neuronal responses are modulated (Corry, 2006)

More than 300 different ion channels surround a cell membrane and they are classified according to their gating property, pore number and the specific type of the ion pass through the channel (Gabashvili *et al.,* 2007, Tabassum and Feroz, 2011). Ligand gated ion channels are generally found in synapse and gated in response to the binding of cytoplasmic messengers or neurotransmitters in order to generate electrical signal by using chemical signals (Harmar *et al.*, 2009). On the other hand, voltage gated ion channel activation requires the specific voltage for the removal of a block that prevents ion flux. Unless voltage or ligand condition is met, conformational change is not induced to open the gate. Voltage gated ion channels have particularly important roles in neuronal communication as well as muscle contraction since they provide quick depolarization upon voltage change. There are also other types of channels such as mechanoreceptors which are gated in response to pressure (Corry, 2006, Aidley and Stanfield, 1996). Another characteristic of ion channels is their selectivity for ions. Size, electrostatic interactions and molecular arrangement in the pore are the key points of selectivity of ion channels.

Some ion channels are controlled by GPCRs either through physical interaction or signalling pathways. Especially in mammals longer N and C-tails of ion channels make it possible for modulation via direct interactions (Dascal, 2001). Some of these interactions only established upon activation of both GPCR and ion channels to get the right conformation for the interaction while some of GPCRs anchor ion channels to the membrane by masking their internalization signal. In addition, direct physical interaction might mask phosphorylation sites which could result in activation or inhibition of the ion channel (Bouvier, 2001).

1.1. 1. N-METHYL D-ASPARTATE RECEPTOR (NMDAR)

Glutamate, which is one of the most important neurotransmitters, take its effect through three types of ionotropic glutamate receptors, namely N-methyl D-aspartate (NMDA), α-amino-3-hydroxy-5-methyl-4-isoxazolepropionic acid (AMPA) and Kainate (KA) receptors (Hollmann *et al.,* 1994). Unlike NMDAR, KA and most of AMPA receptors are impermeable to Ca^{2+}. AMPARs can only allow passage of Ca^{2+} if GluR2 is absent in the tetramer. This difference

renders NMDARs the most prominent member of ionotropic glutamate receptors since Ca^{2+} influx is crucial especially for neurons (Huettner, 2003, Vandenberghe *et al.,* 2000) NMDA receptors involved in many important processes such as memory formation, neuronal communication and synaptic plasticity (Köhr *et al.,* 2006, Prybylowski *et al.,* 2004).

1.1.1.1. MOLECULAR STRUCTURE OF NMDAR

NMDA receptors are tetrameric membrane proteins of which subunit composition depends on the location and the function of the receptor. NMDAR subunits, which are the building blocks of NMDA receptors, designates the interaction of the receptor with neighboring proteins, sensitivity to agonists, antagonists, Mg^{+2} and Zn^{+}, receptor trafficing to the synapse and the location in the brain (Cull-Candy *et al*., 2001).

All NMDAR subunits have the similar structure and membrane topology. N terminal domains of all subunits are extracellular and responsible from subunit assembly. After N-terminal domain, the first part of the agonist binding domain comes and this part forms agonist binding domain by creating a pocket with the loop between M3 and M4. Agonist binding site is where co-agonist glycine or D-serine binds to NR1 and NR3 subunits and the neurotransmitter glutamate binds to NR2 subunits. Transmembrane segments and the loops form the pore region. NMDAR subunits contain three transmembrane segments and a reentering loop (P-loop or TM2) between the first and the third transmembrane segments (Figure 1. 1. 1). This loop contributes to the formation of the channel and an asparagine residue within this loop affects the permeability of the channel to calcium as well as the sensitivity to magnesium.

C- terminal domains of NMDAR subunits vary in length and implicated in the trafficking and interaction of the receptor with other proteins (Paoletti *et al.,* 2011, Sanz Clemente *et al.,* 2012).

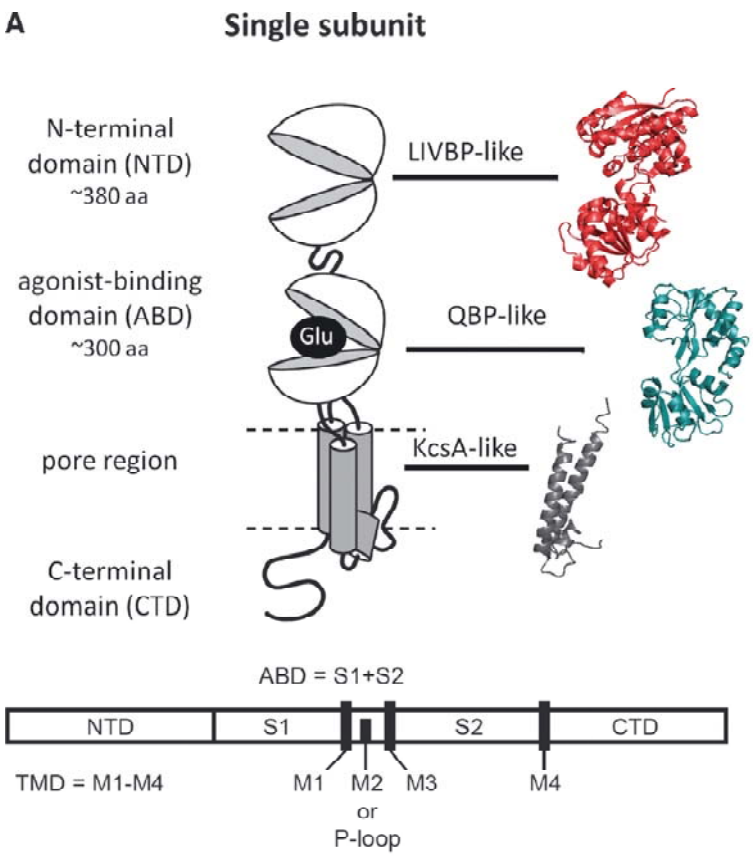

Figure 1. 1. 1. Schematic representation of the membrane topology of a NMDAR subunit (taken from (Paoletti *et al.* , 2011)).

There are mainly three types of NMDAR subunits named as NR1, NR2 (A-D) and NR3 (A,B). For a functional NMDAR receptor to be formed, NR1 has to be involved in the tetrameric structure of the protein. Therefore it is expressed throughout the brain abundantly. However, isoforms show various distribution patterns according to developmental stage and region of the brain (Laurie *et al*., 1994). NR1 has eight isoforms formed by alternative splicing of exons 5, 21 and 22 which are N1, C1 and C2 cassettes respectively (Carroll *et al.,* 2002) (Figure 1. 1. 2).

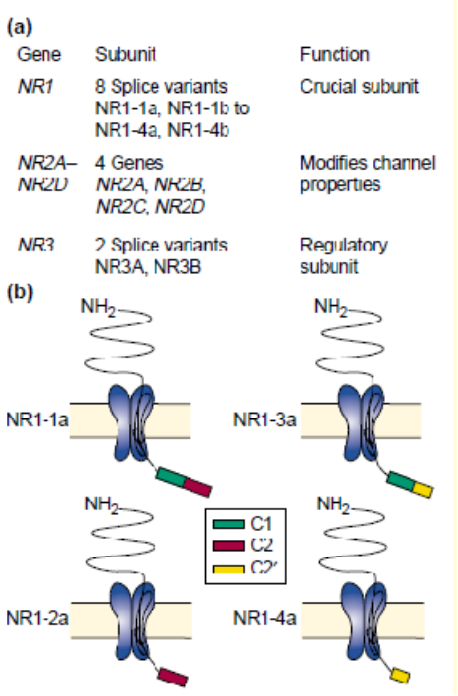

Figure 1. 1.2. (a) Summary of NMDAR subunit isoforms and their main functions. (b) Four important alternatively spliced forms of NR1 subunit (taken from (Carroll *et al.*,2002)).

N1 cassette is extracellular and it is thought to decrease sensitivity to protons by covering the proton sensor of the subunit (Traynelis *et al*., 1995). Presence of N1 cassette also affects deactivation kinetics of NMDA receptors composed of NR1 and NR2B subunits. Receptors having NR1 subunits with N1 cassette are deactivated faster than the ones that do not (Laurie *et al*., 1994). NR1 C terminus has 4 C cassettes, C1 is present in four of the splice variants like C2 and C2' cassettes. C0, C1, C2 and C2' are found in the cytosolic part of the receptor and regulates the interactions with other proteins, such as DREAM, calmodulin, CaMKII, as well as the trafficking of unassembled NR1 subunit. C0 cassette is found in all NR1 isoforms (Wenthold *et al*., 2003, Sanz-Clemente *et al.,* 2012)

Therefore the behaviour of each NMDAR having different NR1 isoforms varies. In the cell there are two separate pools of NR1. The first one forms NMDA receptor by complexing with NR2 or NR3 subunits and delivered to the membrane. The second pool remains unassembled in the ER and this pool has a very short half life. This unstable pool constitutes 45% of all NR1 (Huh *et al*., 1999, Atlason *et al.,* 2007)

There are four types of NR2 subunit as NR2A, NR2B, NR2C and NR2D. Generally the type of NR2 subunit affects the channel properties, proton sensitivity, single channel conductance, open probability, deactivation kinetics, and the interaction with other proteins (Köhr *et al.,* 2006).

NMDA receptors are generally formed as di or triheteromers. NR1/NR2B/NR2D and NR1/NR2B/NR3A compositions are mostly seen in early developmental stages. In adulthood most of these receptors are replaced by NR1/NR2A/NR2B and NR1/NR2A/NR2C complexes due to the synaptic maturation or the activity. In the early developmental stage NR2B containing NMDAR predominates and its level decreases throughout development. Instead, NR2A containing receptors begin to increase after second week of the development and

predominate the synaptic pool in adulthood (Sanz-Clemente *et al*., 2012). This switch has an important role in the decrease of synaptic plasticity (Wenthold *et al*., 2003).
The subunit composition defines the channel property and the location of NMDA receptor (Table 1. 1). Triheteromeric receptors may not show the characteristics of diheteromeric receptors. For example, pure NR1/NR2B and pure NR1/NR2D receptors are generally extrasynaptic however the presence of NR2A subunit in that composition may drive the insertion into the membrane. Likewise, NR1/NR2B/NR2D triheteromeric receptors may not be deactivated as slow as NR1/NR2D diheteromeric receptors (Cull-Candy *et al*., 2001).

Table 1.1. Properties and main distribution of NMDAR composed of two NR1 and two NR2 (A-D) subunits (adapted from (Law *et al*., 2003, Ewald and Cline, 2009, Dravid *et al*., 2008, Cull-Candy, 2001, Mullasseril *et al*., 2010)

	NR2A	NR2B		NR2C	NR2D
Developmental stage (abundant)	Adult	Early		Adult	Early
Distribution	Cortex, hippocampus	Early: Cortex, spinal cord and thalamus	Adult: forebrain	Cerebellum, thalamus, olfactory bulb	Diencephalon, mesencephalon, and spinal cord
Conductance	High	High		Low	Low
Deactivation time	Fast	Medium		Medium	Slow(4-5 sec)
Sensitivity to magnesium	High	High		Low	Low
Synaptic/extrasynaptic	Synaptic	Extrasynaptic		Synaptic	Extrasynaptic
Open probability	High	Low		Low	Low

1.1.1.2. TRAFFICKING OF NMDA RECEPTOR

NMDA receptor subunits are produced by the ribosomes on the ER and signal sequence directs them to ER. The ER retention motif RRR found in the C1 cassette of NR1 subunit causes the

retention of the subunit in the ER unless it is masked. Masking of this motif is achieved by the assembly of NR1 with NR2 or NR1 isoforms other than NR1-1. Only NR1-1 isoform having C0, C1 and C2 cassettes subjected to this rule. Although NR1-3 isoforms have C1 cassette and thus RRR motif, PDZ binding domain -STVV- which is present in C2' cassette interacts with a PDZ protein and drives the forward trafficking of NR1-3. The other isoforms (1-2a, 1-2b, 1-4a and 1-4b) don't contain ER retention signal and they are readily trafficked to the membrane with the help of other proteins that will be mentioned later (Carroll *et al*., 2002, Prybylowski *et al.,* 2004).

Similarly NR2 subunits can not achieve to exit from ER when they are unassembled. NR2 subunits assemble with NR1 subunit through N terminus of NR1 by forming disulfide bonds between cysteines in endoplasmic reticulum and mask ER retention signal found in the C terminus of NR1 (Lee *et al*., 2011).

When N terminus of NR1 is truncated, surface expression of NR2 subunits is abolished. Similarly, when the N terminus of NR1 is replaced with the N terminus of GluR1, NMDARs cannot be delivered to the synapse (Meddows *et al.*, 2001). This experimental finding suggests that the assembly of NMDAR subunits is sequence specific.

There are two scenarios for the assembly of NMDA receptors. The first one is the dimer of homodimers which suggest that two NR1 form homodimer and constitute a tetrameric complex by assembling with a dimer consist of NR2 or NR3 subunits (Schorge *et al*., 2003).

According to the second hypothesis NMDARs assemble in four steps, i. NR1 form homodimers in the absence of NR2 or NR3, ii. Availability of NR2 or NR3 causes the disassembly of NR1 homodimers, iii. NR2 or NR3form heterodimer with NR1, iv. Two heterodimers assembled to form tetrameric NMDA receptor (Farina *et al.,* 2011)

Trafficking of NMDARs are regulated by several motifs. These motifs enable ER retention of unassembled subunits, exit of the assembled receptor from ER and interaction with the proteins which mediates the forward trafficking of NMDAR.

ER retention motif is found on the C terminus of each subunit and prevents the delivery of the unassembled subunits to the membrane. On the other hand, EHLFY motif found at the beginning of C terminus of NR2B promotes the exit of NR2B containing receptor from ER. This motif is EHL for NR2A and EHLVY for NR2C and NR2D (Yang *et al*., 2007, Hawkins *et al*., 2004).

Truncation of three amino acids after TM4 of NR2 subunits prevents the surface delivery of assembled receptor. Yang *et al.* suggest that any three amino acids placed after TM4 overcome the retention. Moreover replacement does not disrupt the functionality of the receptor (Yang *et al.*, 2007).

The TVV motif found in the C2' cassette of NR1 subunit mediates the ER exit of NMDA receptor by interacting with COPII and directs it to Golgi (Kim *et al.,* 2004). ESDV motif found in the C-terminus of NR2 is thought to recruit PSD-95, PSD-93, SAP-97 and SAP102 proteins for the delivery of the receptor to the membrane. PSD-95, PSD-93, SAP-97 and SAP-102 share a common structure by possessing three PDZ, one SH3 and Guanylate Kinase domains. The subunits which have the specific PDZ binding domain bind to corresponding protein. NR2 subunits bind to PSD-95, SAP102 and PSD-93 whereas NR1-4 isoform can bind to all four proteins due to the sequence at its C-terminus (Wenthold *et al.,* 2003). For the formation of the exocyst complex that delivers the receptor to the membrane, additional proteins are recruited such as Sec8 and mPins. In addition to Sec8 and mPins, m-Lin-2, m-Lin-7, m-Lin-10 and KIF 17 proteins are involved in the trafficking of NMDARs. m-Lins and KIF-17 are associated with cargo vesicles in order to deliver NR2 containing receptors to the dendrites and eventually to the synaptic site. These proteins also play role in the trafficking of NR2B containing receptors to the extrasynaptic site (Sans *et al*., 2003, Sans *et al*., 2005, Setou *et al*., 2000, Guillaud *et al*., 2003).

The receptors without PDZ binding domain are not included in the exocyst complex instead they reach to the cell surface with a different mechanism.

Internalization of NMDAR is mediated by PSD-95 and phosphorylation status of tyrosine motifs. The receptors that are not interacting with PSD-95 are less stable and readily internalized. Phosphorylation of the tyrosine at 1472th position of NR2B also contributes to the internalization of NR2B containing NMDARs due to the disruption of the interaction between NR2B and PSD-95. Moreover, YEKL motif and dephosphorylated tyrosine motif at the end of TM4 can bind to AP2 and signals for clathrin mediated endocytosis of NMDAR (Roche *et al*., 2001, Vissel *et al*., 2001).
In the light of these informations, when NR1 or NR2B is transfected to N2a cells alone, we expect to see an ER localized signal as shown in Figure 1.1.3.

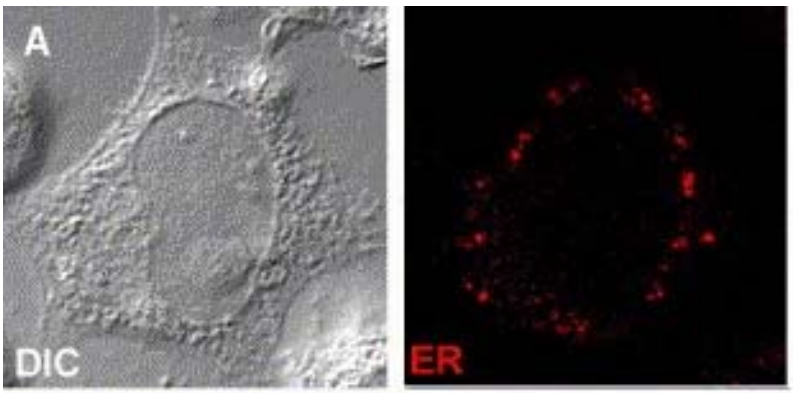

Figure 1.1.3. Confocal microscope image of an N2a cell transfected with ER organelle marker (taken from Hippe *et al*., 2006).

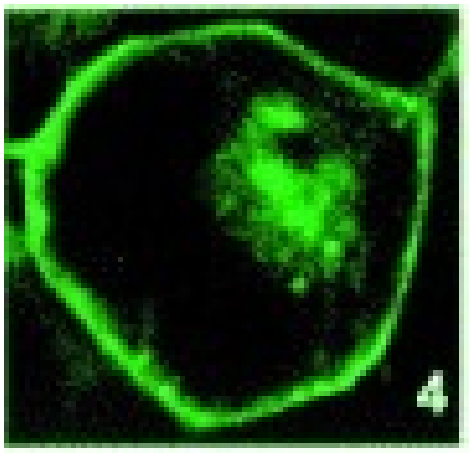

Figure 1.1.4. Confocal microscope image of G-protein coupled glutamate receptor. By considering the literature we expect to see a similar pattern in localization of NMDA receptor (Doherty et. al, 1999).

1.1.1.3. NMDAR SIGNALLING

NMDARs differ from other ion channels because they are both ligand and voltage gated. Activation of NMDAR requires, binding of glycine and glutamate as well as removal of Mg^{2+} block. Upon removal of Mg^{+} block and binding of glutamate and glycine, NMDARs activated and took cations inside the cell. Especially Ca^{2+} influx leads to the initiation of important signal transduction cascades such as memory formation, synaptic plasticity and learning (Furukawa *et al*., 2005). The direction of the cascade initiated by Ca^{2+} influx depends on the subpopulation of NMDARs. Activation of NR2B containing NMDARs, which are mainly found extrasynaptic, induces Long Terminal Depression (LTD) where the activation of synaptic NR2A containing NMDARs induce LTP (Liu *et al.,* 2004). This difference is caused by the frequency of NR2B and NR2A containing channels. NMDARs composed of NR1 and NR2A subunits have a higher frequency of axonal stimulation thus their activation results in Long Term Potentiation (LTP). On the other hand, NR2B containing receptors lead to LTD due to their lower frequency (Yashiro and Philpot, 2008).

1.1.1.3.1. LONG TERM POTENTIATION (LTP)

In basal state, NMDARs are inactive because of Mg^{2+} block. For the removal of Mg^{2+} block a strong afferent stimulation is required. Upon LTP induction Mg^{2+} block is removed due to strong depolarization (Soderling *et al.,* 2000). Besides SRC-family tyrosine kinases further activates NMDARs by phosphorylating them. This causes increased Ca^{2+} influx through NMDARs which in turn increases the level of Ca^{2+}-CaM complex. Interaction of Ca^{2+}-CaM complex with CaMKII leads to autophosphorylation and activation of CaMKII (Lu *et al*., 1998). Activated CaMKII causes potentiation of AMPA receptor which results in LTP.

1.1.1.3.2. LONG TERM DEPRESSION (LTD)

LTD is induced by a weak stimulation which in turn causes weak depolarization of the cell and partial removal of the block on NMDAR. Induction of LTD by NMDAR relies on the activation of a phosphatase cascade which dephosphorylates and causes endocytosis of AMPAR. LTD causes decrease in efficacy of neuronal cells and lasts hours or longer. It is the opposing process of long term potentiation.

1.1.1.3.3. APOPTOSIS

NMDARs not only take role on learning and memory but also on survival and apoptosis. Apoptosis is the programmed cell death which is regulated by many pathways. Upon trigger of

apoptosis caspases act and DNAses degrade DNA of the cell. This process is followed by activation of macrophages and clean up of cellular remainings.
First 3 postnatal weeks are important in terms of NMDAR dependent survival. In many neuron types of developing rats even short periods of NMDAR inhibition induces apoptosis by decreasing ERK1/2 and CREB acitivity of which constitutive activation enhances cell survival. NMDAR antagonist administered animals show learning and memory deficits at a later age (Ikonomidou *et al*., 1999, du Bois *et al*., 2008, Hansen *et al*., 2004). Despite their neuroprotective activity, hyperfunction of NMDARs result in excitotoxicity due to excess Ca^{2+} influx. Thus it is important to balance NMDAR's activity for neuronal health. Potential diseases that may be caused by NMDAR alterations in higher state organisms are shown on Table 1. 2.

Table 1.2. The disorders caused by the imbalance in NMDAR expression.(taken from (Sanz-Clemente *et al*, 2012).

Disorder	NMDAR Alteration
Alzheimer's disease	Reduction in NR2B surface expression Pathological activation of extrasynaptic NMDARs
Parkinson's disease	NR2B redistribution from synaptic to extrasynaptic sites Increased synaptic NR2A
Huntington's disease, Ischemia and stroke	Increased extrasynaptic NMDAR activity
Schizophrenia	Decreased NMDAR function Altered NR2A trafficking via neuregulin/ErbB4 receptor
Alcohol abuse	Decreased synaptic NR2A expression following acute ethanol treatment Increase in NMDAR currents following chronic ethanol treatment
Cocaine abuse	Elevated insertion of NR2A following acute cocain treatment Increased AMPAR-NMDAR ratio after repeated cocaine administration

1.2. IMMUNOCYTOCHEMISTRY

There are several methods to identify the presence of a specific protein in a cell such as western blot, fluorescent tagging and FACS. However sometimes it is required to detect the localization of a protein in a cell without affecting its mobility and trafficking. Immunocytochemistry is the only method which can identify the localization of a protein without affecting its cellular localization and mobility. In our case we have used ICC in order to compare the trafficking of recombinant receptors with wild type N2a cell line receptors.
Basically upon fixation of the cells primary antibody which is raised against the antigen of interest is applied on the fixed preparation in order to provide site for binding of the secondary antibody. For the generation of a fluorescent image secondary antibody needs to be tagged.

Tagging of secondary antibody can be achieved through conjugating a fluorescent tag to the secondary antibody, conjugating an enzyme which develops color up on exposure to its substrate, biotinylating the secondary antibody which in turn binds to fluorophore labelled avidin or biotinylated enzyme. Since biotin have four molecular binding sites, it gives three times more signal than non-biotinylated taggings. Thus biotinylated secondary antibodies can be used effectively in detection of sensitive immunocytochemical stainings.

1.3. AIM OF THE STUDY

In this study, firstly we aimed to show distribution of NMDARs in mouse neuroblastoma cell line (N2a) by fusing it with EGFP and mCherry fluorescent proteins from the end of C-terminal tail of NMDAR subunits. We also aimed to confirm membrane and ER localized distribution of NMDAR with this strategy. While detecting the distribution pattern of NMDARs we also tested the fate of NMDAR subunits when transfected without its counter subunits and fate of NR2B subunit when transfected with truncated NR1 subunit which has only N terminal domain.

Moreover by changing the position of the fluorescent tag we wanted to determine the effect of labeling position on NMDAR distribution and signal strength of EGFP and mCherry proteins.

In the context of this study, wild type mouse NMDARs found in the untransfected N2a cells were tagged by using immunocytochemistry method in order to be able to compare the distribution pattern of EGFP and mCherry labelled human NMDARs in N2a cells.

In conclusion this study aims to reveal the distribution pattern of NMDARs in N2a neuronal cell line and to determine the effect of fluorescent protein labeling on the distribution of NMDARs.

When the effect of NMDAR on many pathological processes such as schizophrenia, Alzheimer's disease, Parkinson's disease, alcohol abuse, cocaine abuse, Huntington's disease, ischemia and stroke is considered, it is important to construct an *in vitro* system in order to model the involvement of NMDAR in these processes and to detect the effect of drugs targeting NMDAR related pathways in molecular level when combined to a functional assay for detection of NMDAR activity. This is especially important for schizophrenia since the number of the drugs affecting the interaction between dopamine D2R and NMDARs are increasing day by day. By using the constructs prepared in this study it can be possible to detect the efficiency of the drugs targeting D2R-NMDAR interactions by means of Förster's Resonance Energy Transfer (FRET) technique.

CHAPTER II

MATERIALS & METHODS

2.1. MATERIALS

2.1.1. NEURO2A (N2A) MOUSE NEUROBLASTOMA CELL LINE AND MEDIA

EGFP and mCherry tagged constructs were transiently transfected to normal N2a cell line (generous gift by Assist. Prof. Dr. Tülin YANIK, METU Biological Sciences, Ankara, Turkey) to observe the proteins.
N2a cells were grown for three days in N2a cell media containing 10% Fetal Bovine Serum (Invitrogen, Cat#26140-079), 1% Penicillin/Streptomycin solution (Invitrogen, Cat#15140-122), 44.5% Dulbecco's Modified Eagle Medium (D-MEM) with L-glutamine (Invitrogen, Cat#41966029) and 44.5% OPTIMEM®I Reduced Serum Medium with L-glutamine (Invitrogen,Cat#31985047). N2a media was sterilized by filtrating through Millipore Stericup® Filter Unit.

2.1.2. MAINTENANCE OF N2A CELL LINES

N2a cells were grown in their growth medium for about 72 hours at 37 ^{o}C with 5% CO_2 in Heraeus® Hera Cell 150 Tri-Gas Cell Culture incubator to reach 90% confluency. After three days their growth medium was removed and cells were washed with PBS solution of which composition is given in Appendix A. Na_2HPO_4, KH_2PO_4, NaCl and KCl were dissolved in distilled water and pH was adjusted to 7.4. Then, 1X PBS solution was sterilized by autoclaving at 121^{o}C for 20 minutes. After washing, cells were lifted from the cell culture flask by 1ml of TrypLE™ Express Stable Trypsin like Enzyme with Phenol Red (Invitrogen, Cat#12605-028). Detached cells are taken from the flask by adding 9 ml cell media and 10% of cells were transferred into a new T-75 flask containing 16 ml cell media.
For stocking of the cells, 10^7 cells were centrifuged at 1000 rpm for 5 minutes and resuspended in 1 ml of freezing medium containing 35% DMEM, 35% OPTIMEM®I, 20% glycerol and 10 % FBS. Then the cells were kept in -80 ^{o}C for 24 hours before taking them into nitrogen tank for storage. For the revival of stocks, cryovials were incubated at 37 ^{o}C, transferred to 15 ml falcon tube by adding 9 ml cell growth medium and centrifuged at 1000 rpm for 5 minutes. Then the cells were resuspended in fresh growth medium and transferred to cell culture flask.

2.1.4. BACTERIAL CULTURE MEDIA AND CONDITIONS

Escherichia coli TOP 10 cells were grown in Luria Bertani (LB) Medium. LB medium and LB plates were prepared as explained in Appendix B and autoclaved at 121 ^{o}C for 20 minutes for sterilization. For the selection of ampicillin or kanamycin resistant bacteria 1 mL of 100 mg/mL ampicillin or 50 mg/mL kanamycin was added to LB medium containing agar after it cooled down to ~50 ^{o}C. Bacteria were grown on the plates at 37 ^{o}C in Nüve® incubator. In order to select ampicillin or kanamycin resistant bacteria in liquid broth, 500 µg of ampicillin or kanamycin was added to 5 ml of LB and grown at 37 ^{o}C in Zheiheng shaker incubator.
Bacterial stocks are prepared by mixing 50% sterile glycerol and liquid bacterial culture in 1:1 ratio and stored in -80 ^{o}C.

2.1.5. OTHER MATERIALS

The chemicals used in this study were purchased from Merck (Darmstadt, Germany), Applichem (Darmstadt, Germany) and Sigma Chemical Company (NY, USA). Restriction enzymes and DNA ligases were purchased from New England Biolabs (Hertfordshire, UK), Fermentas (Ontario, Canada) and Roche Molecular Biochemicals (Basel, Switzerland). DNA polymerases were from Fermentas (Ontario, Canada), Finnzymes (Vantaa, Finland) and New England Biolabs (Hertfordshire, UK). Plasmid isolation, gel elution and PCR purification kits were from QIAGEN (Düsseldorf, Germany) and Fermentas (Ontario, Canada). Cell culture media, serum and other cell culture reagents were purchased from GIBCO®, Invitrogen (CA, USA). Antibodies used in immunocytochemistry were from Abcam (Cambridge, UK). Primers are synthesized by Alpha DNA (Quebec, Canada). Sigma MK-801 NMDAR antagonist was kindly gifted by Assist. Prof. Dr. Hakan Kayır.
Receptor clones were purchased from Gene Copoeia (PA, USA) and Imagene. Enhanced Green Fluorescent Protein (EGFP) and mCherry cDNA were generous gifts from Prof. Dr. Henry Lester, California Institute of Technology, CA, USA.
Fluorescent images were obtained by Zeiss 510 laser scanning microscope and Leica DMI 4000 fluorescence microscope.

2.2. METHODS

2.2.1. PREPARATION OF COMPETENT E.COLI CELLS

2.2.1.1. PREPARATION OF COMPETENT *E.COLI* CELLS BY $CACL_2$ METHOD

TOP 10 strain of *E.coli* was used for all competent cell preparations. TOP 10 cells were streaked onto LB agar plate and incubated overnight at 37 ^oC. A single colony was inoculated into 5 ml LB medium and incubated with shaking overnight at 37 ^oC. Next day, 5 ml culture was added to 50 ml LB and incubated at 37 ^oC in a shaker incubator for about two hours to an OD_{600} nm of 0.48-0.75. If the condition was met, the bacterial culture was transferred to a 50 ml falcon tube and incubated on ice for 15 minutes. Then it was centrifuged at 4100 rpm for 7 minutes at 4 ^oC. Supernatant was removed and the pellet was dissolved in 15 ml 0.1 M sterile ice cold $CaCl_2$ solution and incubated on ice for 15 minutes. After this, it was centrifuged again at 4100 rpm for 7 minutes at 4 ^oC. Supernatant was removed and the pellet was dissolved in 4 ml, 0.1 M sterile ice cold $CaCl_2$ + 15% glycerol solution. Then 100 µl aliquots of this bacterial solution was frozen in liquid nitrogen and stored at -80 ^oC.

2.2.1.2. PREPARATION COMPETENT *E.COLI* CELLS BY $RBCL_2$ METHOD

A single colony was picked from TOP 10 plate that was streaked on the previous day, inoculated in 5 ml LB medium and incubated overnight with shaking at 37 ^oC. Next day the bacterial culture was added to 100 ml LB and grown at 37 ^oC shaker incubator until OD_{600nm} was between 0.48 and 0.75. Then the culture was divided in two 50 ml falcon tubes and incubated on ice for 5 minutes. After incubation on ice, the culture was centrifuged at 6000 rpm for 5 minutes at 4 ^oC. Supernatant was discarded and the pellet was resuspended in 20 ml ice cold TfbI of which composition is given in Appendix C. This bacterial solution was incubated on ice for 5 minutes and centrifuged again at 6000 rpm for 5 minutes at 4 ^oC. Supernatant was removed and pellet was dissolved in 2 ml ice cold TfbII. Composition of TfbII is given in Appendix C. Bacterial solution was chilled on ice for 15 minutes and distributed in 100 µl aliquots. Aliquots were frozen in liquid nitrogen and stored in the -80 ^oC freezer.

2.2.2. TRANSFORMATION OF COMPETENT E.COLI CELLS

E.Coli TOP10 cells made competent before and stored in -80 ^oC freezer were taken and incubated on ice for 10 minutes. 50-100 ng plasmid or 10 µl ligation / dNTP digestion reactions were added on the competent cells. DNA and competent cell mixture was chilled on ice for 30 minutes. During incubation on ice, heat block was adjusted to 42 ^oC and after 30 minutes cells were heat shocked at 42 ^oC for 90 seconds. Upon heat shock cells were incubated on ice for 5 minutes. Then 800 µl of prewarmed LB was added on the cells and bacteria were grown at 37 ^oC for 1 hour by inverting them at every 10 minutes. After that, cells were

centrifuged at 6000 rpm for 3 minutes. 700 µl of the supernatant was removed and the cells were resuspended in the remaining 100 µl supernatant. Finally cells were spreaded on the LB agar plate containing the antibiotic which the plasmid transformed was resistant to. Plates were incubated at 37 ^{o}C overnight.

2.2.3. PLASMID ISOLATION FROM *E.COLI* CELLS

A single colony from the agar plate was picked and inoculated into 5 ml liquid LB medium containing 1 µl of the antibiotic which the plasmid was resistant to. The bacterial culture was incubated overnight at 37 ^{o}C in a shaker incubator. Next day the plasmids were isolated by using Fermentas® GeneJET Plasmid Miniprep Kit according to manufacturer's instructions.

2.2.4. RESTRICTION ENZYME DIGESTION

All digestion reactions in this study were prepared as 20 µl reactions. Suggested digestion reaction buffer (listed in Appendix C), 1.5 µg of DNA, 8 unit of the restriction enzyme, dH_2O up to 20 µl and if required BSA was added to the reaction. Then the reaction was incubated at 37 ^{o}C for at least two hours.

2.2.5. *IN VITRO* LIGATION

After digestion of the plasmid and the insert with compatible restriction enzymes, digestion reaction was run on 0.8% agarose gel and the DNA at desired size was eluted from the gel. Purified DNA was used to set ligation reaction. For ligation reaction, 1 unit of T4 DNA ligase (Roche Applied Science, Cat#10481220001), 1X T4 DNA ligase buffer, DNA to be ligated and dH_2O up to 20 µl was added. Plasmid and the insert was added in 1:10, 1:20 or 1:50 ratio regarding their sizes and incubated at room temperature overnight.

2.2.6. POLYMERASE CHAIN REACTION (PCR)

PCR method was used to add restriction enzyme cut sites to each ends of the NMDAR subunits in order to clone the receptor clones into pCDNA 3.1(-) vector. NheI-NotI and NotI-AflII cut

sites were added to the upstream and downstream of NR1 and NR2A genes respectively. Optimized PCR condition for this purpose is tabulated in Table 2.1.

Table 2.1. Optimized PCR conditions to generate restriction enzyme cut sites

Reagents	Amount
Template	100 ng
Phire Buffer (5X)	10 µl
$MgCl_2$	1 µl
dNTP (25 mM)	1 µl
Forward Primer (20 pmol)	1 µl
Reverse Primer (20 pmol)	1 µl
DMSO	1 µl
Phire Hot Start II DNA Polymerase	1 µl
Nuclease Free Water	Completed up to 50 µl

	NR1
Pre Denaturation- 98 ^oC	30 sec
Denaturation- 98 ^oC x 36	5 sec
Annealing- 54 ^oC x 36	5 sec
Extension-72 ^oC x 36	1 minute
Final extension-72 ^oC	1 minute

Besides, PCR was used to amplify fluorescent protein genes EGFP and mCherry by adding 30 bp flanking ends which would be used in PCR integration method. Optimized PCR conditions for fluorescent protein amplification are shown on Table 2.2.

Table 2.2. Optimized PCR conditions for fluorescent protein amplification

Reagents	Amount
Template	150 ng
Taq Buffer (10X)	5 µl
$MgCl_2$	4 µl
dNTP (25 mM)	1 µl
Forward Primer (20 pmol)	1 µl
Reverse Primer (20 pmol)	1 µl
Taq DNA Polymerase	0.3 µl
Nuclease Free Water	Completed up to 50 µl

	NR1	
Pre Denaturation- 96 ^oC	5 min	
Denaturation- 96 ^oC	30 sec	} 35 cycles
Annealing- 53 ^oC	45 sec	
Extension-72 ^oC	1 min	
Final extension-72 ^oC	5 min	

2.2.7. AGAROSE GEL ELECTROPHORESIS

In order to control the size of DNA which was amplified by PCR or digested before, agarose gel electrophoresis was used. To run the DNA smaller than 1 kb, 1% agarose gel was prepared in TBE buffer where the DNA longer than 1 kb was run on 0.8% agarose gel. After melting the agarose in microwave oven, ethidium bromide (EtBr) was added on the gel to intercalate and stain the DNA under UV light. Then it was let to solidify on the tray after placing combs on it. Then combs were taken and DNA sample which was mixed with 6X loading dye (Fermentas®, Cat#R0611) in 1:5 loading dye to DNA ratio was loaded in the wells. The gel was run in TBE buffer at 100V for 35-40 minutes.

2.2.8. EXTRACTION OF DNA FROM AGAROSE GEL

DNA at the correct size was excised from the gel and extracted by using QIAGEN® Gel Extraction Kit (Cat#28704) according to the manufacturer's instructions.

2.2.9. MEASUREMENT OF DNA AMOUNT

1 µl of the DNA sample to be measured was loaded on NanoDrop 2000 spectrophotometer (Thermo Scientific®) and quantified by using NanoDrop 2000 software.

2.2.10. PCR INTEGRATION METHOD

Receptors are tagged with fluorescent proteins by using PCR integration method. This method is based on the integration of the first PCR product which was amplified to be flanked by 30 bp upstream and downstream of targeted site. The first PCR product was extracted from agarose gel and used as primer in the second PCR in 1:5 template to insert ratio. pCDNA 3.1(-) vector containing the receptor gene was used as the template and the whole vector containing the desired insert was amplified in second PCR. Then PCR reaction was digested with DpnI enzyme to digest the template which was methylated and digestion reaction was transformed to *E.coli* to amplify the PCR product.

Table 2.3. PCR conditions for PCR integration method

Reagent	Amount
Template	70 ng
1st PCR Product	350 ng
Phire® Reaction Buffer	10 µl
DMSO	1 µl
dNTP	1 µl
Phire® DNA Polymerase	1 µl
Nuclease Free Water	Completed up to 50 µl

98°C for 30 sec

98°C for 30 sec

51°C for 1 min

68°C for 2 min/kb

} 18 cycles

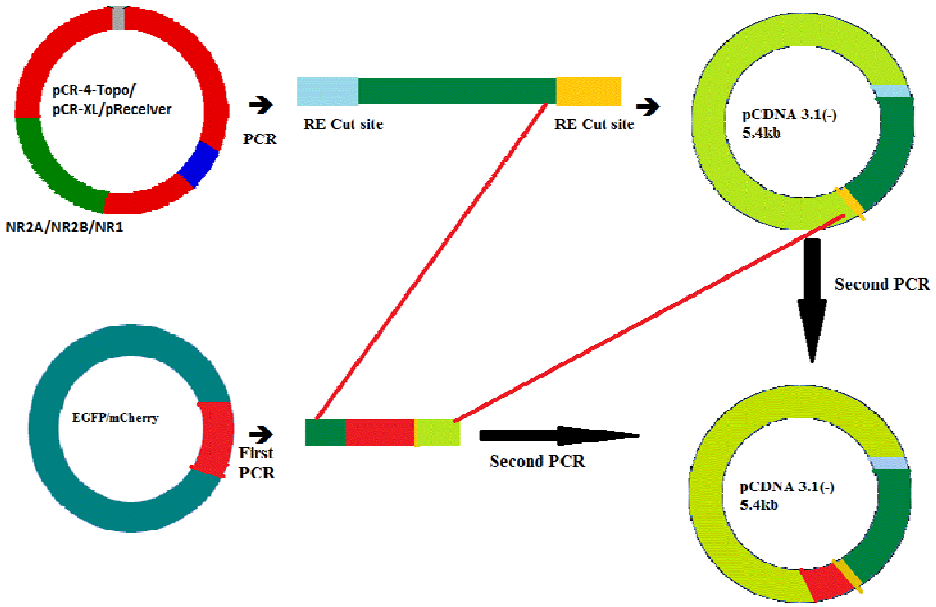

Figure 2.1. Summary of fluorescent tagging of receptors. Upon cloning of NR1 and NR2B subunits to pCDNA 3.1 (-) mammalian expression vector, EGFP and mCherry fluorescent protein genes were amplified to insert overhangs for its insertion to the region of interest.

2.2.11. CORRECTION OF THE MUTATIONS WITH SITE DIRECTED MUTAGENESIS METHOD

After sequencing of the cloned and flurescent tagged receptor genes, mutations and deletions were detected. For correction of the mutations and insertions, site directed mutagenesis primers with 7-9 bp overlap between forward and reverse primers were designed. While designing forward primers, 3-4 bp upstream and 15-17 bp downstream of the site that would be mutated was taken. Reverse primers were designed by taking 3-4 bp downstream and 15-17 bp upstream of the site that would be mutated and the primer was converted to its reverse complement. Then the whole vector was amplified by PCR. Optimized site directed mutagenesis conditions are shown on table 2.4.

Table 2.4. Optimized site directed mutagenesis conditions

Reagent	Amount
Template	100 ng
Forward Primer (20 pmol)	1.5 µl
Reverse Primer (20 pmol)	1.5 µl
Phire® Reaction Buffer	10 µl
DMSO	1 µl
dNTP	1 µl
Phire® DNA Polymerase	1 µl
Nuclease Free Water	Completed up to 50 µl

98°C for 30 sec

98°C for 30 sec

51°C for 1 min

68°C for 2 min/kb

18 cycles

Then PCR reaction was digested with DpnI enzyme to digest the template which was methylated and digestion reaction was transformed to *E.coli* to amplify the PCR product.

2.2.12. TRANSFECTION OF N2A CELLS WITH PCDNA 3.1 (-) VECTOR

In the first day of transient eukaryotic transfection, 50.000 N2a cells were seeded on each glass bottom dish. Then cells were let to grow for 24 hours and next day the plasmid and 6 µl of Plus Reagent was added in 100 µl of OPTIMEM® I. For NMDAR expression, 3 µg from each NMDAR subunit was added into the mixture. After incubation of the mixture at room temperature for 15 minutes, OPTIMEM® I and Lipofectamine LTX™ mixture containing 50 µl of OPTIMEM® I and 4 µl of Lipofectamine LTX™ was added on the first mixture and incubated at room temperature for 15 minutes. During this time previously seeded cells were washed with 1X PBS and 0.9 ml OPTIMEM® I was added on the cells. After the last 15 minute

incubation, the mixture was added on the cells and the dishes were swirled 2-3 times. Then the cells were incubated for 3 hours at 37 ^{o}C in 5% CO_2. Finally after 3 hours incubation 1 ml growth medium with serum was added on the cells and dishes were put back to the incubator for expression of the receptors.

2.2.13. LOCALIZATION OF NR1 AND NR2B SUBUNITS IN N2A CELLS WITH IMMUNOCYTOCHEMISTRY

Immunocytochemistry was applied to both transfected and and untransfected cells. To detect the localization NR1 and NR2B subunits in transfected cells with immunocytochemistry, 50.000 cells were seeded on glass bottom dishes in the first day. Next day transient transfection protocol was followed and cells were left to produce NR1 and NR2B subunits for 48 hours. Immunocytochemistry protocol can be started on fourth day for transfected cells. For detection of wild type NR1 and NR2B subunits in N2a cells, 90.000 cells were plated in the first day and next day immunocytochemistry protocol was started by fixation with 2% formaldehyde solution. Preparation of formaldehyde solution is shown in Appendix C. For fixation, cell culture medium was removed and 600 µl of formaldehyde solution was added and incubated for 20 minutes at room temperature. After incubation cells were washed twice with 1X PBS and rinsed with 800 µl of wash buffer (Appendix C). Upon rinsing 800 µl blocking buffer (Appendix C) was added and incubated at room temperature for 45 minutes. During this time primary antibodies were diluted in 1:5000 ratio with dilution buffer (Appendix C). After incubation cells were covered with primary antibody and incubated at room temperature for 1 hour. While waiting for the binding of primary antibody, secondary antibody was diluted in 1:500 ratio. After incubation cells were washed twice with wash buffer and cells were covered with secondary antibody. From this point on cells were protected from light. Then cells were incubated at room temperature for 1 hour. Finally cells were washed once with wash buffer, once with 1X PBS and once with molecular grade water. Dishes can be imaged by exciting at 590 nm immediately or can be kept at 4 ^{o}C up to 3 months.

CHAPTER III

RESULTS AND DISCUSSION

3.1. RESULTS

3.1. 1. CLONING OF NMDAR CODING SEQUENCES TO PCDNA 3. 1 (-) VECTOR

First of all, cDNAs of NMDAR subunits were transferred into pcDNA 3.1 (-) vector to make a consensus between copy numbers, selection and other experimental conditions. Unfortunately we could not find appropriate cut sites for NR1 and NR2A clones. So we designed primers to add appropriate cut sites to 5' and 3' ends of these subunits.

3.1.1.1. CLONING OF NR1 SUBUNIT INTO PCDNA 3. 1 (-) VECTOR

To be able to insert NR1 gene between *NheI* and *NotI* cut sites within multiple cloning site of pCDNA 3.1 (-) eukaryotic expression vector, GCTAGC sequence was added to 5' end and GCGGCCGC sequence was added to 3' end of NR1 coding sequence. In addition, to provide extra sites for higher restriction enzyme efficiency any four bases were added to 5' ends of primers. Primers are shown below:

Forward Primer: 5' – ATACGCTAGCACCATGAGCACCATGCGCC – 3'
Reverse Primer: 5' – ATACGCGGCCGCCACCACGGTGCTGACCGA – 3'

After amplification of NR1 coding sequence with cut site addition primers, PCR products were run on 0.8% agarose gel (Figure 3.1.1.1) and the DNA in the correct size was eluted from the gel.

Figure 3. 1. 1. 1. PCR product of NR1 coding sequence flanked with *NheI* and *NotI* cut sites run on 0.8 % agarose gel. 1. High range DNA ladder. 2. NR1 with restriction enzyme sites (2680 bp).

PCR product that was eluted from agarose gel and pCDNA 3.1 (-) vector was digested with *NheI* and *NotI* enzymes. In order to prevent further sample loss, digested NR1 was purified with PCR purification kit. pCDNA 3.1 (-) vector was run on 0.8 % agarose gel (Figure 3. 1. 1. 2) and extracted by using gel extraction kit.

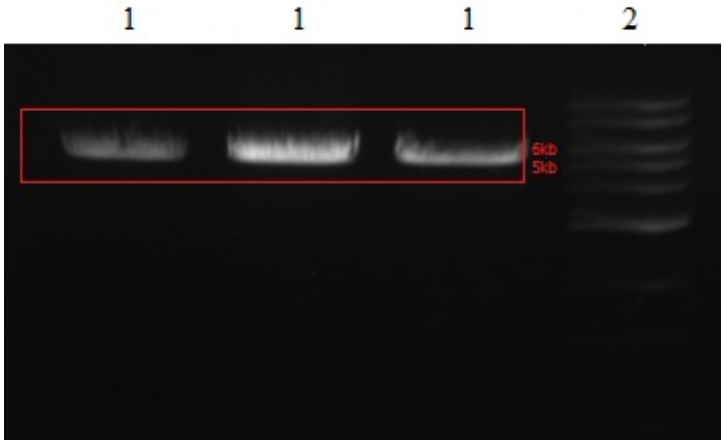

Figure 3. 1. 1. 2. pCDNA 3.1(-) vector was digested with *NheI* and *NotI* enzymes for its ligation with NR1 and run on 0.8% agarose gel.1. Digested pCDNA 3.1 (-) vector. 2. NEB 1kb ladder.

Concentrations of purified NR1 and pCDNA 3.1 (-) digests were measured and mixed in 1:20 and 1:50 vector to insert ratio. Then *in vitro* ligation reaction was prepared by addition of T4 DNA ligase and its buffer. Ligation reaction was incubated at room temperature for three hours and transformed to *E.coli.* 10 colonies were isolated and digested with *NheI* and *NotI* enzymes for confirmation of presence of the insert (Figure 3. 1. 1. 3. and Figure 3. 1. 1. 4.). Two of the isolated plasmids were shown to contain NR1 coding sequence and sequenced for further confirmation.

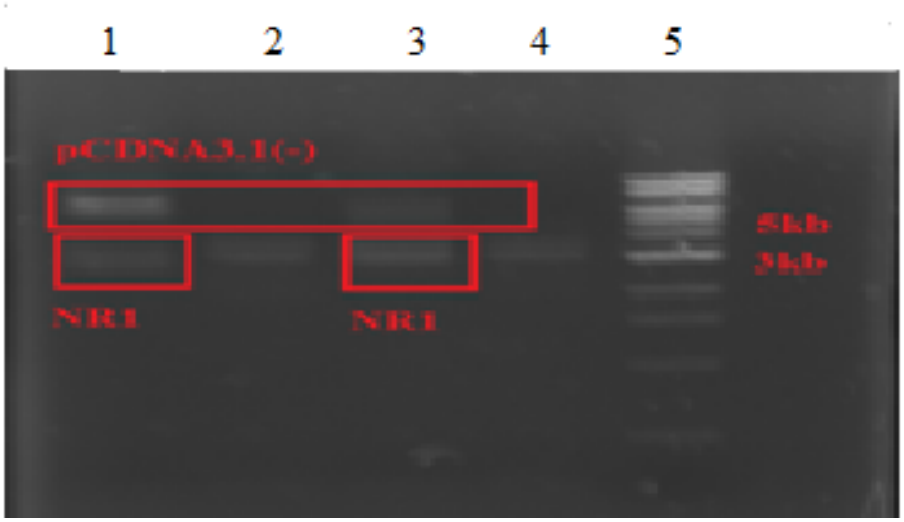

Figure 3. 1. 1. 3. Plasmids that were isolated after NR1-pCDNA 3.1 (-) ligation were controlled with *NheI-NotI* digestion.1.Colony 1, 2. Colony 2, 3. Colony 3, 4. Colony 4, 5. NEB 1kb DNA ladder.

GTCAATGACGGTAAATGGCCCGCCTGGCATTATGCCCAGTACATGACCTTATGGGACTTTCCTACTTGG
CAGTACATCTACGTATTAGTCATCGCTATTACCATGGTGATGCGGTTTTGGCAGTACATCAATGGGCGT
GGATAGCGGTTTGACTCACGGGGATTTCCAAGTCTCCACCCCATTGACGTCAATGGGAGTTTGTTTTGG
CACCAAAATCAACGGGACTTTCCAAAATGTCGTAACAACTCCGCCCCATTGACGCAAATGGGCGGTAGG
CGTGTACGGTGGGAGGTCTATATAAGCAGAGCTCTCTGGCTAACTAGAGAACCCACTGCTTACTGGCTT
ATCGAAATTAATACGACTCACTATAGGGAGACCCAAGCTGGTTAGCACCATGAGCACCATGCGCCTGCT
GACGCTCGCCCTGCTGTTCTCCTGCTCCGTCGCCCGTGCCGCGTGCGACCCCAAGATCGTCAACATTGG
CGCGGTGCTGAGCACGCGGAAGCACGAGCAGATGTTCCGCGAGGCCGTGAACCAGGCCAACAAGCGGCA
CGGCTCCTGGAAGATTCAGCTCAATGCCACCTCCGTCACGCACAAGTC

Figure 3. 1. 1. 4. Presence of NR1 coding sequence in pCDNA 3.1 (-) vector was confirmed by sequencing. Black letters refers to pCDNA 3.1 (-) where blue letters refers to NR1 coding sequence.

3.1.1.2. CLONING OF NR2B SUBUNIT INTO PCDNA 3.1 (-) VECTOR

In original vector of NR2B (pCR-XL-TOPO) (Figure 3. 1. 1. 5) there were two *EcoRI* cut sites at upstream and downstream of NR2B cDNA. So NR2B subunit cDNA was simply cloned into pCDNA 3.1 (-) vector by digesting and ligating.

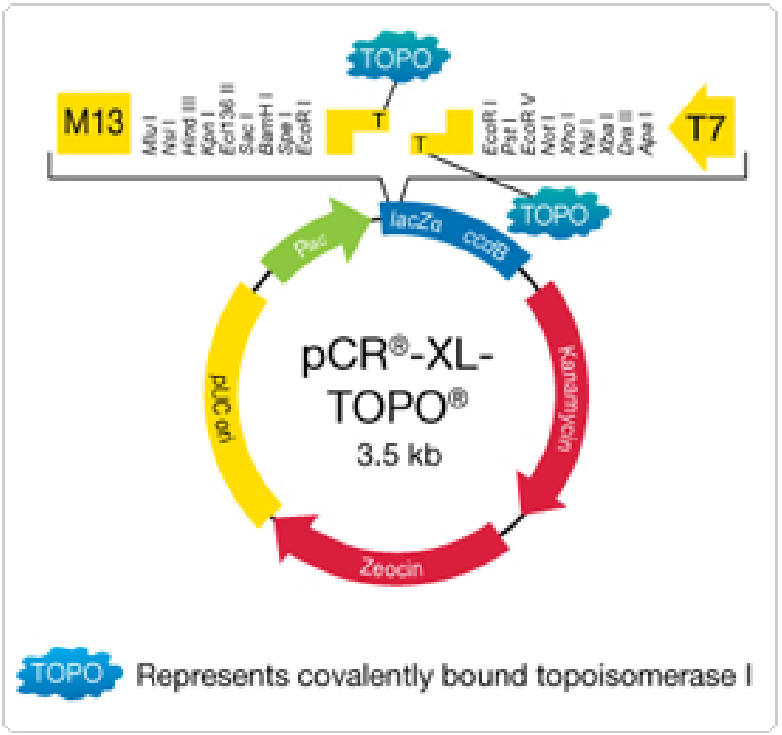

Figure 3. 1. 1. 5. NR2B was originally found in pCR-XL-TOPO vector. In order to transfer it to pCDNA 3.1 (-) vector, it was digested with EcoRI enzyme.

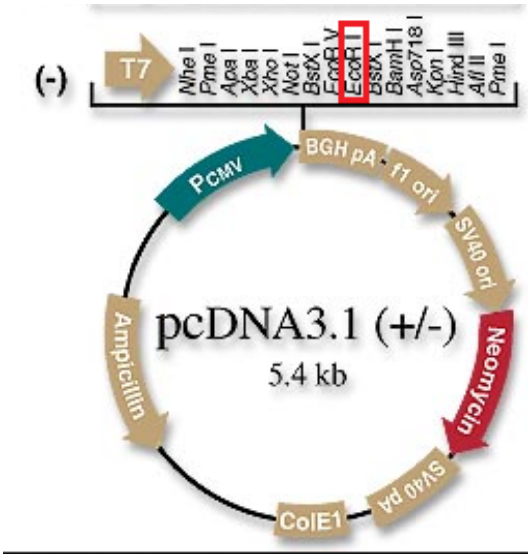

Figure 3. 1. 1. 6. NR2B subunit gene was ligated in EcoRI site which is shown in red box.

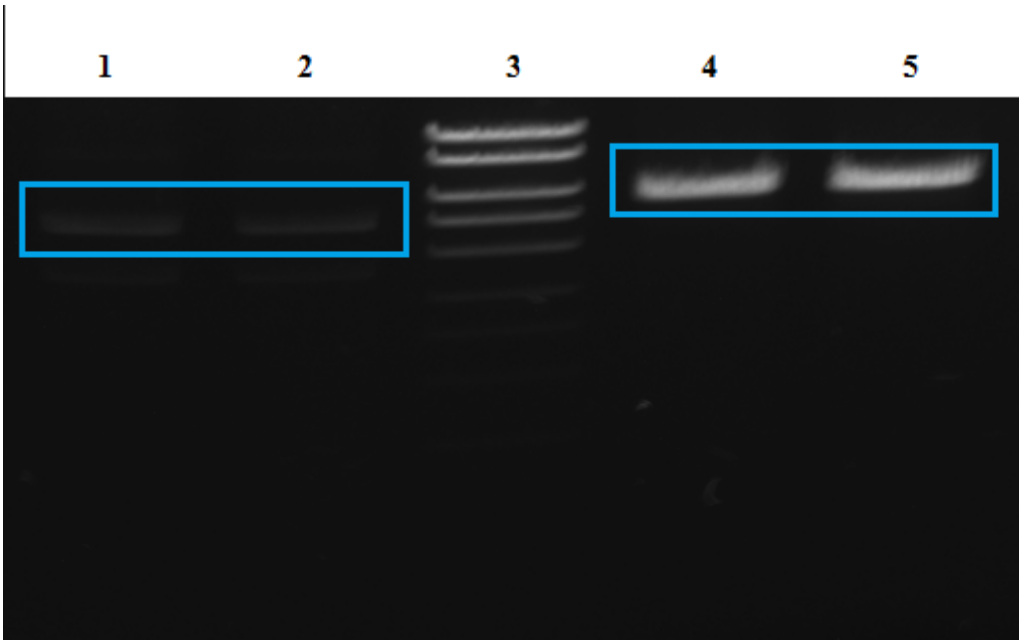

Figure 3. 1. 1. 7. 2B cDNA was digested with *EcoRI* enzyme for cloning into pCDNA 3.1 (-) vector. 1&2. NR2B in pCR-XL-TOPO vector. 3. High Range DNA ladder. 4&5. pCDNA 3.1 (-) vector.

Size of the desired plasmid was confirmed by *NotI* digestion and direction of the insert was checked by sequencing (Figure 3. 1. 1. 8).

CAATGACGGTAAATGGCCCGCCTGGCATTATGCCCAGTACATGACCTTATGGGACTTTCCTACTTGGCA
GTACATCTACGTATTAGTCATCGCTATTACCATGGTGATGCGGTTTTGGCAGTACATCAATGGGCGTGG
ATAGCGGTTTGACTCACGGGGATTTCCAAGTCTCCACCCCATTGACGTCAATGGGAGTTTGTTTTGGCA
CCAAAATCAACGGGACTTTCCAAAATGTCGTAACAACTCCGCCCCATTGACGCAAATGGGCGGTAGGCG
TGTACGGTGGGAGGTCTATATAAGCAGAGCTCTCTGGCTAACTAGAGAACCCACTGCTTACTGGCTTAT
CGAAATTAATACGACTCACTATAGGGAGACCCAAGCTGGCTAGCGTTTAAACGGGCCCTCTAGACTCGA
GCGGCCGCCACTGTGCTGGATATCTGCAGAATTCGCCCTTTTCCCAACATGCTCACTCCCTTAATCTGT
CCGTCTAGAGGTTTGGCTTCTACAAACCAAGGGAGTCGACGAGTTGAAGATGAAGCCCAAGAGCGGAGT
GCTGTTCTCCCAAGTTCTGGTTGGTGTTGGCCGTCCTGGGCCGTGTC

Figure 3. 1. 1. 8. Presence of NR2B sequence in pCDNA 3.1 (-) vector was confirmed by sequencing. Black letters refers to pCDNA 3.1(-) where blue letters refers to NR1 coding sequence.

3.1.2. TAGGING NMDAR WITH MCHERRY AND EGFP BY USING PCR INTEGRATION METHOD

3.1.2.1. TAGGING NR1 SUBUNIT WITH MCHERRY AND EGFP BY USING PCR INTEGRATION METHOD

For EGFP and mCherry labelling of NR1 subunit, primers were designed to flank EGFP and mCherry genes with the last 30 bp of the receptor and the first 30 bp of the pCDNA 3.1 (-) vector after *NotI* cut site. Because the stop codon of NR1 subunit was removed while transferring it to pCDNA 3.1 (-) vector, this primer does not contain stop codon.
Forward Primer:
5'- ctctcagatccctcggtcagcaccgtggtgATGGTGAGCAAGGGCGAGGAG- 3'
Reverse Primer:
5'- attctgcagatatccagcacagtggcggccTTACTTGTACAGCTCGTCCATGCC- 3'
Lowercases at the beginning of the primers represent the integration sites and added to each side of EGFP and mCherry genes after the first cycle. In the first cycle only the bases shown in uppercase binds to the template.

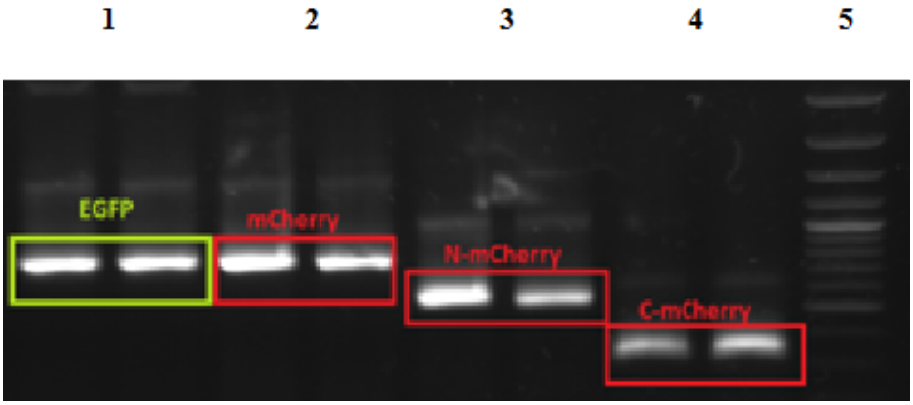

Figure 3.1.2.1. mCherry and EGFP genes were amplified with PCR in order to add overhangs to enable insertion of EGFP and mCherry to the template.1. EGFP with NR1 overhangs. 2. mCherry with NR1 overhangs. 3&4. Split mCherry parts with NR1 overhangs. 5. Fermentas 100 bp plus DNA ladder.

EGFP and mCherry with NR1 overhangs were extracted from agarose gel and used in the second PCR reaction (Figure 3.1.2.1.). Colonies that were grown after transformation of secon PCR product were inoculated and plasmids were isolated. Plasmids were firstly controlled with PCR (Figure 3.1.2.2. and Figure 3.1.2.3.) and then with sequencing (Figure 3.1.2.4. and Figure 3.1.2.5.) for the presence of the insert.

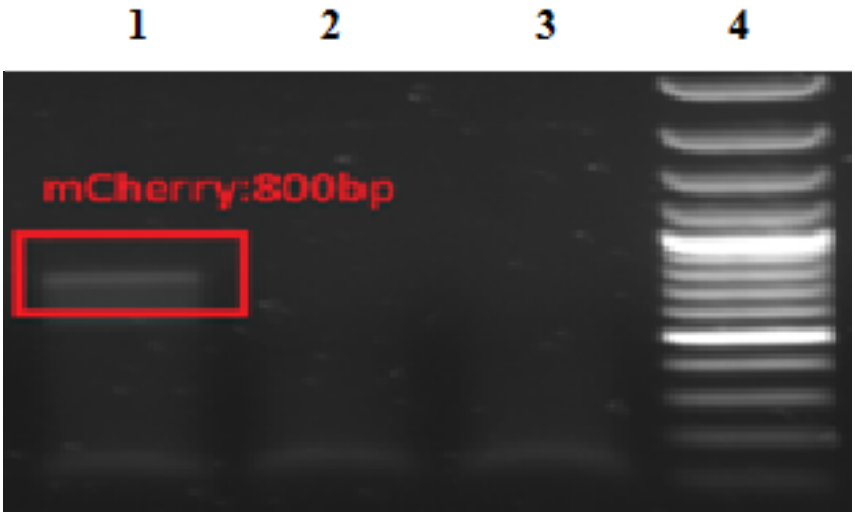

Figure 3.1.2.2. Plasmids were controlled with PCR for the presence of mCherry gene inside the vector. 1, 2 and 3 represents the colony numbers. Fermentas 100 bp plus DNA ladder was loaded on the fourth lane.

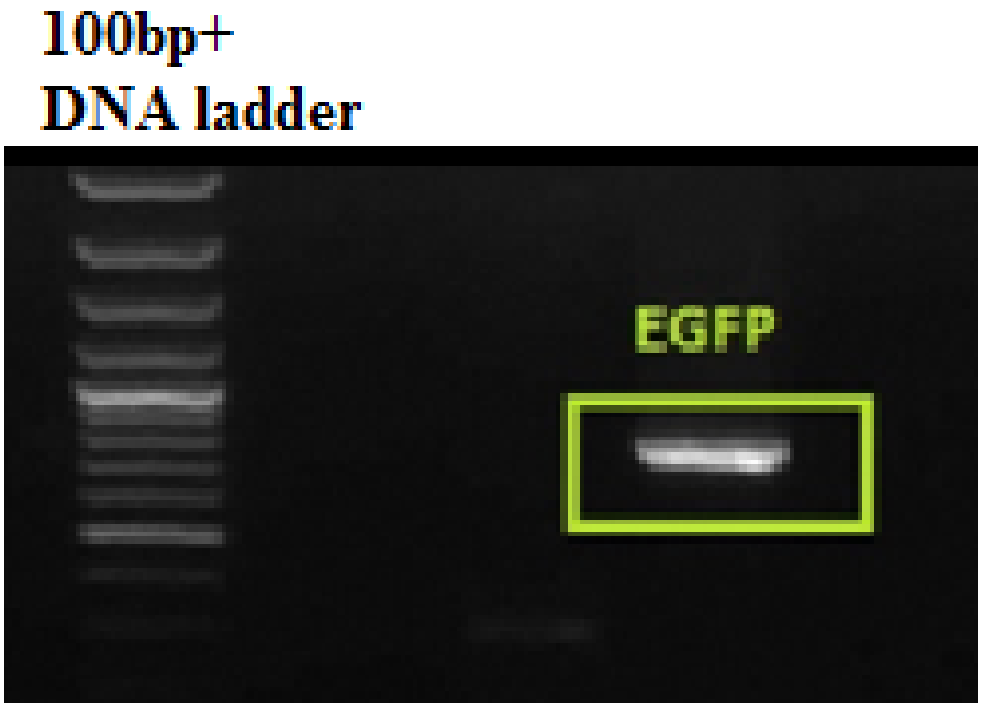

Figure 3.1.2.3. Plasmids were controlled with PCR for the presence of EGFP gene inside the vector. EGFP band shown in green box shows the success of PCR integration method.

GGATCTTCCTGATTTTCATCGAGATTGCCTACAAGCGGCACAAGGATGCTCGCCGGAAGCAGATGCAGC
TGGCCTTTGCCGCCGTTAACGTGTGGCGGAAGAACCTGCAGCAGTACCATCCCACTGATATCACGGGCC
CGCTCAACCTCTCAGATCCCTCGGTCAGCACCGTGGTGATGGCCCGCCTGGCTGACCGCCCAACGACCC
CCGCCCATTGACGTCAATAATGACGTATGTTCCCATAGTAACGCCAATAGGGACTTTCCATTGACGTCA
ATGGGTGGACTATTTACGGTAAACTGCCCACTTGGCAGTACATCAAGTGTATCATATGCCAAGTACGCC
CCCTATTGACGTCAATGACGGTAAATGGCCCGCCTGGCATTATGCCCAGTACATGACCTTA

Figure 3. 1.2.4. Presence of EGFP at the right place and frame was confirmed by sequencing. Black bases represent NR1 coding sequence and red bases represent EGFP.

GGATCTTCCTGATTTTCATCGAGATTGCCTACAAGCGGCACAAGGATGCTCGCCGGAAGCAGATGCAGC
TGGCCTTTGCCGCCGTTAACGTGTGGCGGAAGAACCTGCAGCAGTACCATCCCACTGATATCACGGGCC
CGCTCAACCTCTCAGATCCCTCGGTCAGCACCGTGGTGATGGTGAGCAAGGGCGAGGAGGATAACATGG
CCATCATCAAGGAGTTCATGCGCTTCAAGGTGCACATGGAGGGCTCCGTGAACGGCCACGAGTTCGAGA
TCGAGGGCGAGGGCGAGGGCCGCCCCTACGAGGGCACCCAGACCGCCAAGCTGAAGGTGACCAAGGGTG
GCCCCCTGCCCTTCGCCTGGGACATCCTGTCCCCTCAGTTCATGTACGGCTCCAAGGCCTACGTGAAGC
ACCCCGCCGACATCCCCGACTACTTGAAGCTGTCCTTCCCCGAGGGCTTCAAGTGGGAGCGCGTGATGA
ACTTCGAGGACGGCGGCGTGGTGACCGTGACCCAGGACTCCTCCCTGCAGGACGGCGAGTTCATCTACA
AGGTGAAGCTGCGCGGCAC

Figure 3. 1. 2. 5. Presence of mCherry at the right place and frame was confirmed by sequencing. Black bases represent NR1 coding sequence and the red bases represent mCherry.

After confirming the presence of the insert at the right place, tagged NR1 and untagged NR2B constructs were transiently transfected to N2a cells to form the channel and enable its delivery to the membrane. Although several approaches were tried such as changing concentrations of plasmid DNA from 800 ng to 4 µg, combination with other subunits, imaging at different time points and blocking its activity with MK-801 which is an NMDAR antagonist; we could not get signal from any of the constructs. Thus we thought that it might be because of any point mutation or frameshift and prepared and transfected 6 more NR1-EGFP and 3 more NR1-mCherry constructs. From these constructs, only 2 EGFP and 1 mCherry constructs gave signal when 3µg was transfected. From these constructs, EGFP and mCherry tagged construct gave detectable florescence signal after microscopic imaging. However unlike our expectation, these NR1 subunits were localized all through the cell (Figure 3.1.2.6).

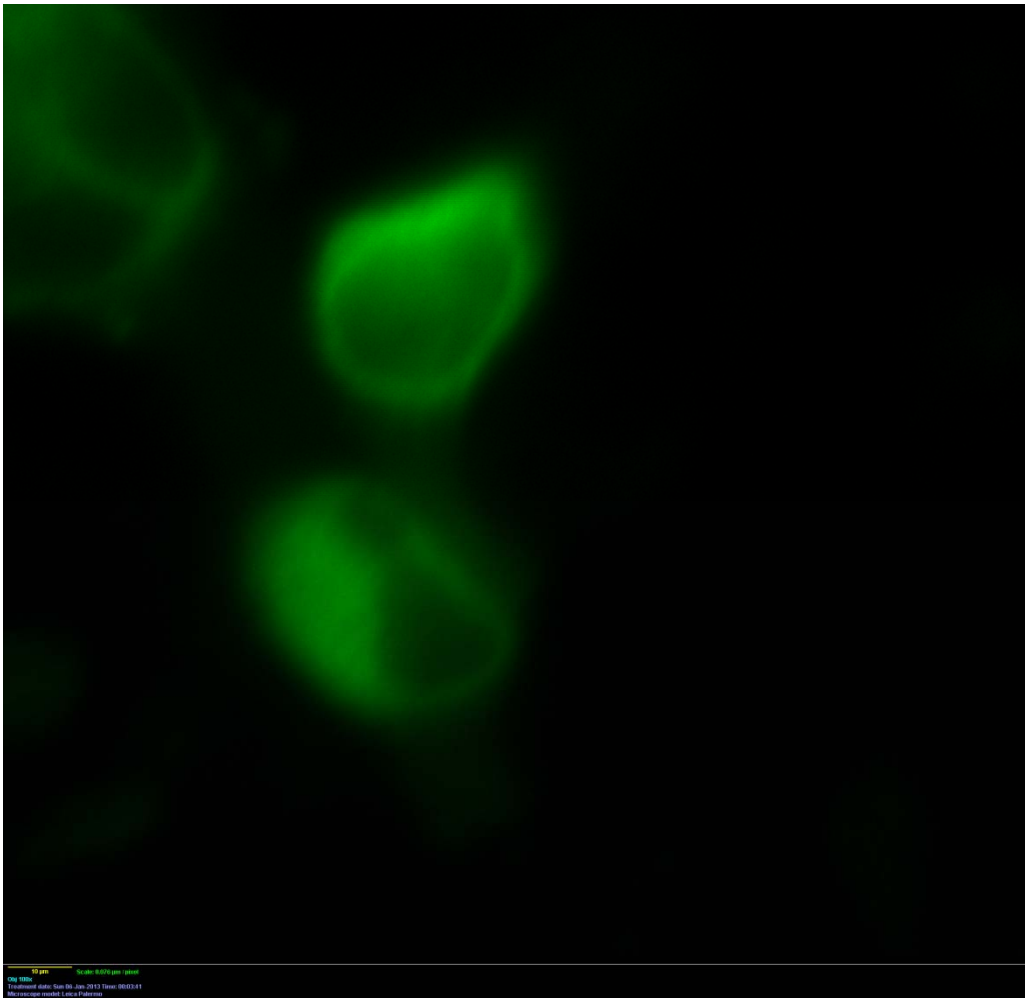

Figure 3.1.2.6. NR1 subunit was transfected to N2a cell line. Unexpectedly cytosolic distribution of EGFP tagged NR1 shows that NR1 does not reside only in the ER when it is transfected without its counter subunits. (100x oil objective).

When the tagged receptors transfected with wild type counter subunits such as wt. NR2B subunit with EGFP tagged NR1 subunit the signal was mostly cytosolic with detectable receptors in cell projections (representing dendrites or axons) as seen in Figure 3.1.2.7.

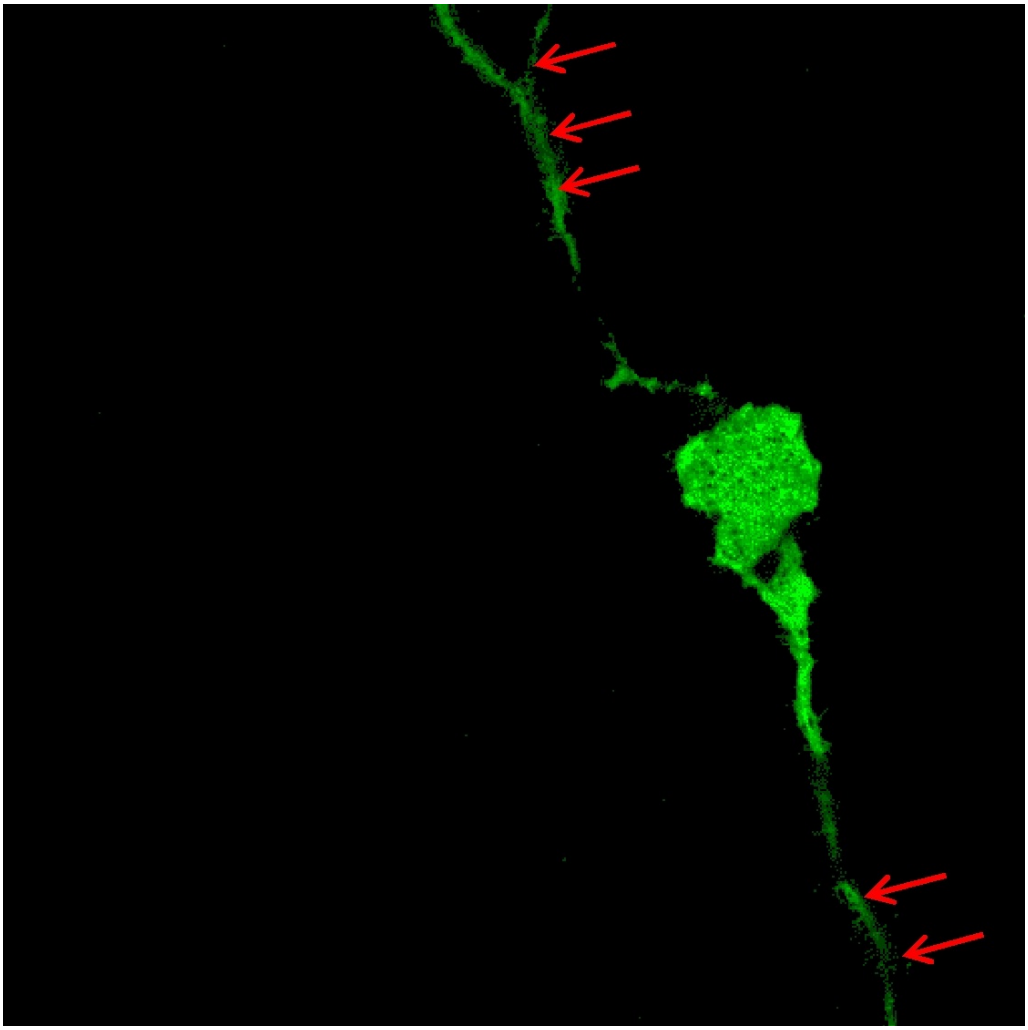

Figure 3.1.2.7. Confocal microscope image of NR1-EGFP and wild type NR2B constructs were transiently transfected into N2a cells EGFP signal is mostly in the cytosol however the cell projections are also visible (marked by red arrows) indicating presence of the tagged receptor in these cell compartments (63x oil objective).

Similarly mCherry tagged NR1 subunit localized mostly in the cytosol (Figure 3.1.2.8.).

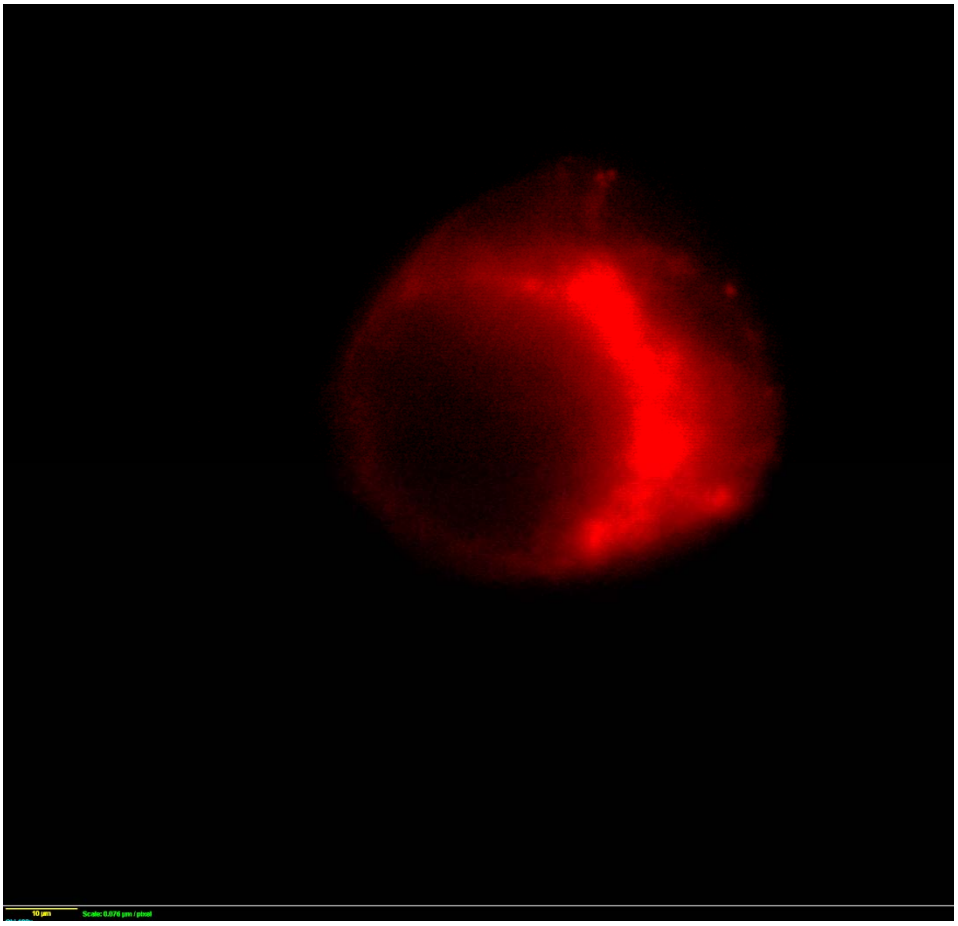

Figure 3.1.2.8. Confocal microscope image of NR1-mCherry and wild type NR2B constructs were transiently transfected into N2a cells mCherry signal is mostly in the cytosol and partially in ER. (63x oil objective).

Unlike our expectations these tagged subunits were mostly cytosolic with some present on the cell surface and cell projections. In order to confirm if this distribution pattern matches with the wild type untagged receptor subunits distribution pattern additional immunocytochemistry experiments were conducted. These studies detailed in section 3.1.3.1 "*Detection of Wild Type NMDAR localization in N2a Mouse Neuroblastoma Cells by Immunocytochemistry*" of this thesis. In summary the immunocytochemistry results showed that these receptors are mostly localized in the cytosol with detectable signal present on the cell membrane.
However due to unexpected localization of these tagged receptors prior to immunocytochemistry studies, alternative tagging strategies were tested. One of the possibilities that could cause trafficking problems was the masking of PDZ domain (up on tagging) which was required for membrane delivery of NMDARs. In order to test this hypothesis an extra PDZ domain was added to the end of EGFP tag. While designing primers to add PDZ domain, *NotI* cut site at the end of EGFP was mutated and we controlled the plasmids by digesting them with *NheI* and *NotI* enzymes. So the plasmids which were not digested with *NotI* enzyme but *NheI* enzyme were the ones that we could mutate and added PDZ domain.

Forward Primer: 5'-
GCATGGACGAGCTGTACGTCAGCACCGTGGTGTAAGAGGCCGCCACTGTGCTGGA
TATCTG- 3'
Reverse Primer: 5'-
CAGATATCCAGCACAGTGGCGGCCTCTTACACCACGGTGCTGACGTACAGCTCGTC
CATGC- 3'
For this purpose, PDZ domain was added to the end of EGFP with PCR integration method and plasmids that were isolated were controlled with *NheI* and *NotI* enzyme digestion for the insertion of PDZ domain (Figure 3.1.2.9).

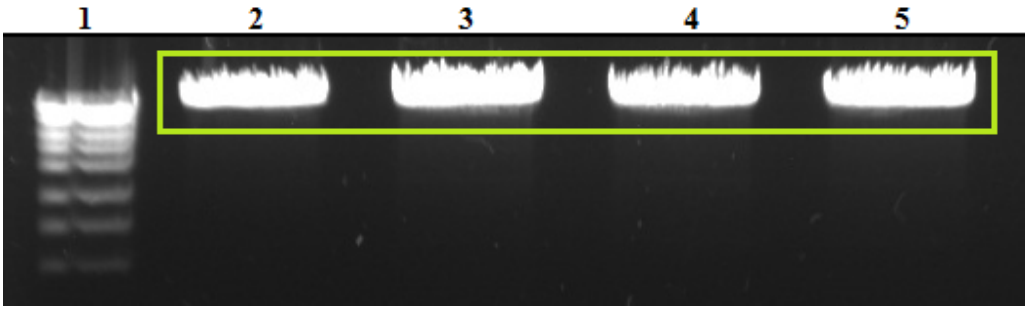

Figure 3.1.2.9. PDZ domain was added to the end of EGFP and controlled by digesting with *NheI* and *NotI*. Since we see only one band, we can say that *NotI* restriction cut site is interrupted due to successful insertion of PDZ domain.

Although, this additional PDZ domain increased the detectable EGFP signal it did not improve the cell surface localization of these receptors (Figure 3.1.2.10).

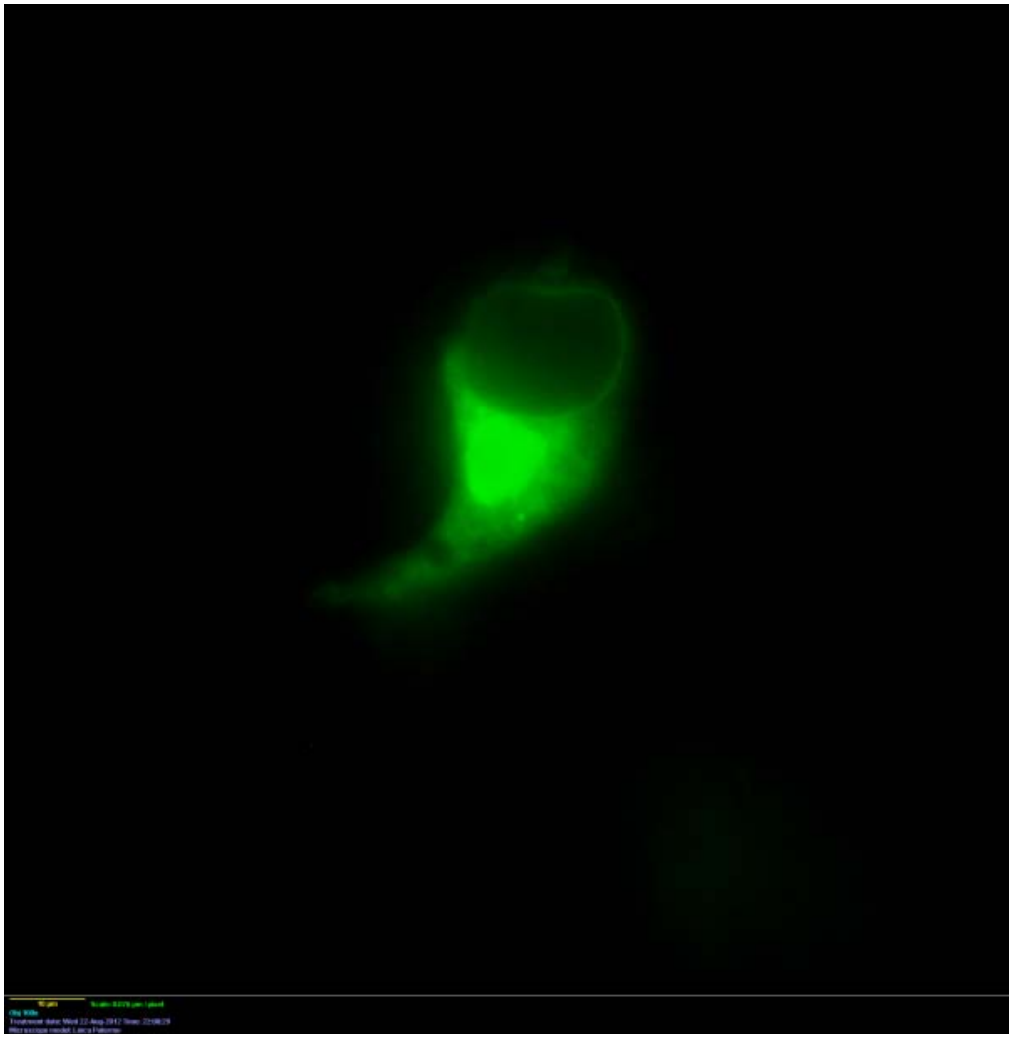

Figure 3.2.10. Fluorescent microscope image of extra PDZ domain added NR1-EGFP and wild type NR2B subunit transfected N2a cell (100 x oil objective). As seen in the image, NMDAR distribution is cytosolic even after addition of PDZ domain. This result suggests that unexpected distribution of NMDAR is not because of PDZ domain masking.

Besides the addition of PDZ domain at the end of the fluorescent tags we tried inserting the tags before the C-terminus of the receptor subunits instead of adding them to the end of the C-terminus tail. For this purpose after analysis of the C-terminus of NR1 gene to avoid possible posttranslational modification motifs, mCherry tag was inserted between the 870^{th} and 871^{st} residues. Possible modification sites were determined by using genome motif finder tool (http://www.genome.jp/tools/motif/) and primers were designed to add EGFP and mCherry to 870^{th} residue. The closest phosphorylation site was 5 residues away from this site.

NR1 870 Forward Primer: 5'-
AACCTGCAGCAGTACCATCCCACTGATATCATGGTGAGCAAGGGCGAGGAG- 3'

NR1 870 Reverse Primer 5'-
CGAGGGATCTGAGAGGTTGAGCGGGCCCGTCTTGTACAGCTCGTCCATGCC- 3'
With these primers, EGFP and mCherry fluorescent protein genes were flanked with overhangs for their insertion to 870th position of NR1 subunit (Figure 3.1.2.11).

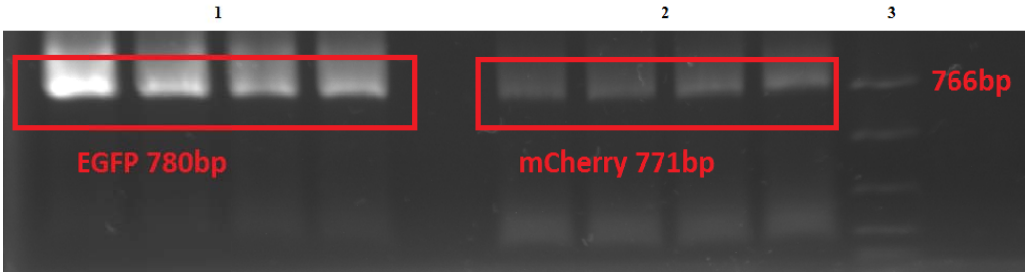

Figure 3.2.11. mCherry and EGFP were amplified by adding flanking sites for their insertion to 870th position.

Image analysis of these tagged receptors had increased membrane localization with significant signal from intracellular compartments (Figure 3.1.2.12).

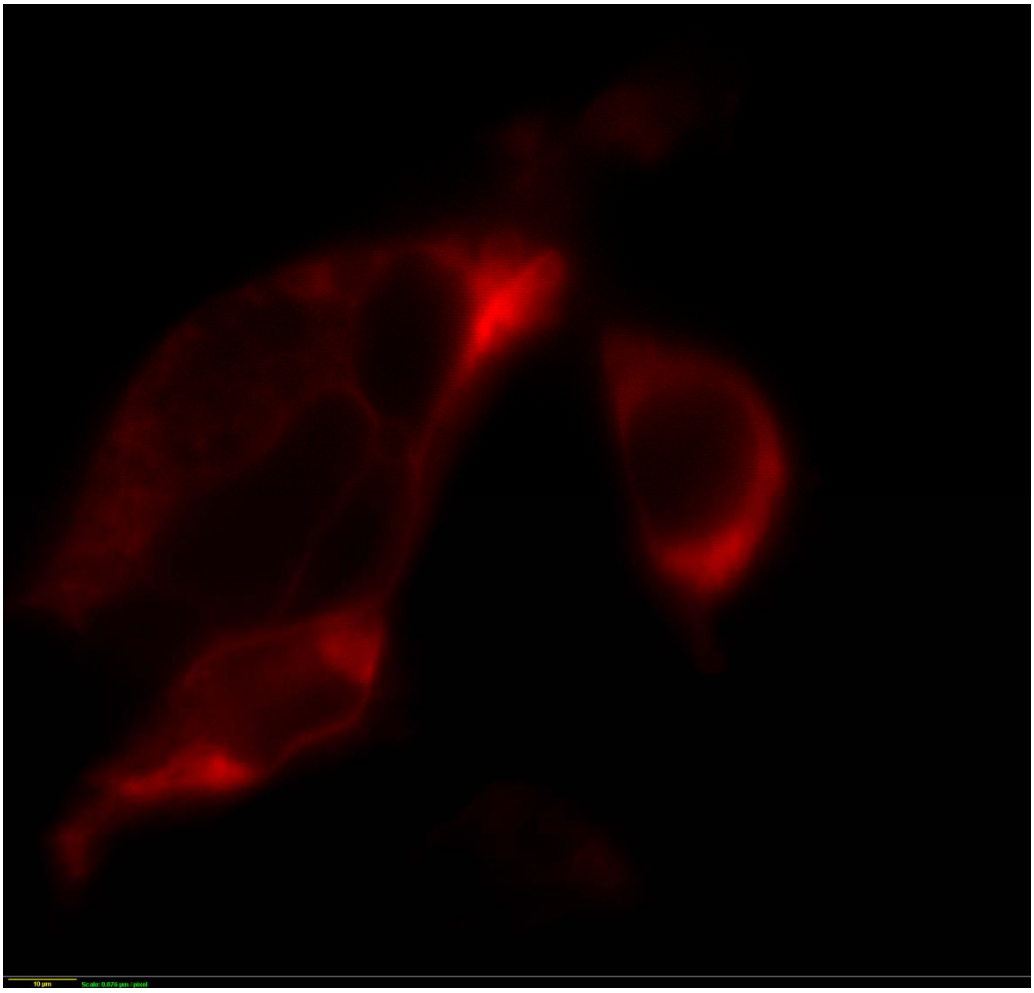

Figure 3.1.2.12. Fluorescent microscope image of NR1 subunit which was tagged from 870th position (100 X oil objective). Image analysis of these tagged receptors had increased membrane localization with significant signal from intracellular compartments.

As a result of multiple tagging strategies and similar localization of all tagged receptor subunits, we decided to carry out immunocytochemistry studies to identify localization of untagged receptors in N2a cell line.
Although NR1 subunit genes was purchased, during confirmation of tagging and insertion in to new expression vector we realized point mutations compared to the sequence submitted in NCBI for this gene. Besides there were mutations introduced during the cloning experiments such as a guanine deletion in NR1 subunit causing a frame shift in the coding sequence. This deletion caused premature termination of NR1 subunit.
Mutations were corrected by site directed mutagenesis.

Primers that were designed for this purpose are as follows:
NR1-1098th Position Site Directed Mutagenesis Forward
Primer: 5'- CTCGGGGAACGCCCTGCGCTAC- 3'

NR1-1098th Position Site Directed Mutagenesis Reverse
Primer: 5'- GTTCCCCGAGATCTCGCGCTC- 3'

Deletion at 1098th base was corrected and confirmed by sequencing. After correction of the deletion at 1098th base, second site directed mutagenesis was done for the mutation at 2048th base. Primers that were designed for this purpose were:

NR1 2048th Position Site Directed Mutagenesis Forward
Primer: 5'-GTGGTGGCCGTGATGCTGTACC-3'

NR1 2048th Position Site Directed Mutagenesis Reverse
Primer: 5'- GGCCACCACGTGCACCGACAGC- 3'

Site directed mutagenesis of this site was controlled with sequencing and finally the last mutation at 580th base was corrected with the primers shown below:
NR1 580th Position Site Directed Mutagenesis Forward
Primer: 5'- CATCTCCAGCCAGGTCTACGCCATC-3'

NR1 580th Position Site Directed Mutagenesis Reverse
Primer: 5'- CTGGAGATGAGGTCCTCGCACAC-3'

3.1.2.2. TAGGING NR2B SUBUNIT WITH MCHERRY AND EGFP BY USING PCR INTEGRATION METHOD

Long C-terminus tail of NR2B mediates important functions and interactions. In addition last five residues which corresponds to PDZ binding domain is ciritically important in membrane delivery of NMDARs. In order to preserve these sites from masking, possible modification sites were determined by using a motif finder tool and primers were designed to add EGFP and mCherry to 972th and 1372th positions.
NR2B 972th Position Forward Primer:
5'ATCAGTGAGGTAGAGAGAACGTTCGGGAACATGGTGAGCAAGGGCGAGGAG3'
NR2B 972th Position Reverse Primer:
5'TTGGTACACGTTGCTGTCCTTCAGCTGCAGCTTGTACAGCTCGTCCATGCC3'
NR2B 1372th Position Forward Primer:
5'CACCACAACAACCCCGGCGGCGGGTACATGATGGTGAGCAAGGGCGAGGAG3'
NR2B 1372th Position Reverse Primer:
5'GACCCGGTCAGGGTAGAGCGACTTGCTGAGCTTGTACAGCTCGTCCATGCC3'

With these primers, EGFP and mCherry fluorescent protein genes were flanked with overhangs for their insertion to 972 and 1372th positions of NR2B subunit (Figure 3.1.2.13 and Figure 3.1.2.14).

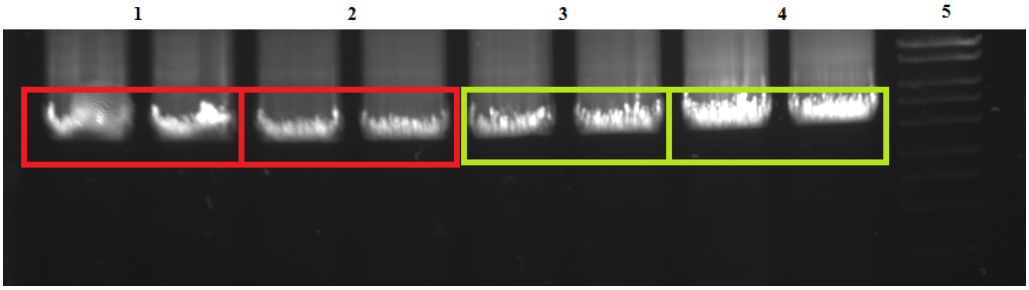

Figure 3.1.2.13. mCherry and EGFP were amplified with PCR by adding flanking sites for their insertion to 972th and 1372th positions of NR2B. 1. mCherry with 972th position overhangs. 2. mCherry with 1372th position overhangs. 3. EGFP with 972th position overhangs. 4. EGFP with 1372th position overhangs. 5. DNA ladder.

After integrating these flanked EGFP and mCherry to their corresponding positions by PCR integration method, plasmids were controlled with PCR (Figure 3.1.2.14, Figure 3.1.2.15, Figure 3.1.2.16) and sequencing (Figure 3.1.2.17, Figure 3.1.2.18, Figure 3.1.2.19 and Figure 3.1.2.20).

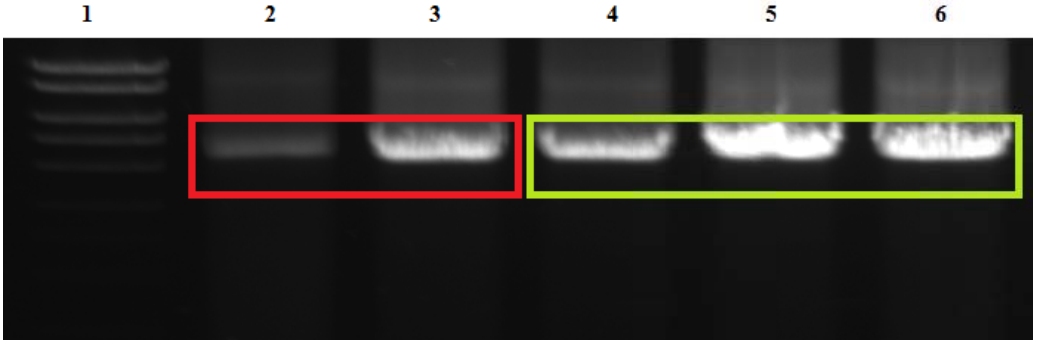

Figure 3.1.2.14. Plasmids were controlled with PCR for the presence of EGFP and mCherry at 972th position of NR2B. 1. DNA ladder, 2. NR2B 972 mCherry-1, 3. NR2B 972 mCherry-2, 4. NR2B 972 EGFP- 1, 5. NR2B 972 EGFP- 2, 6. NR2B 972 EGFP- 3.

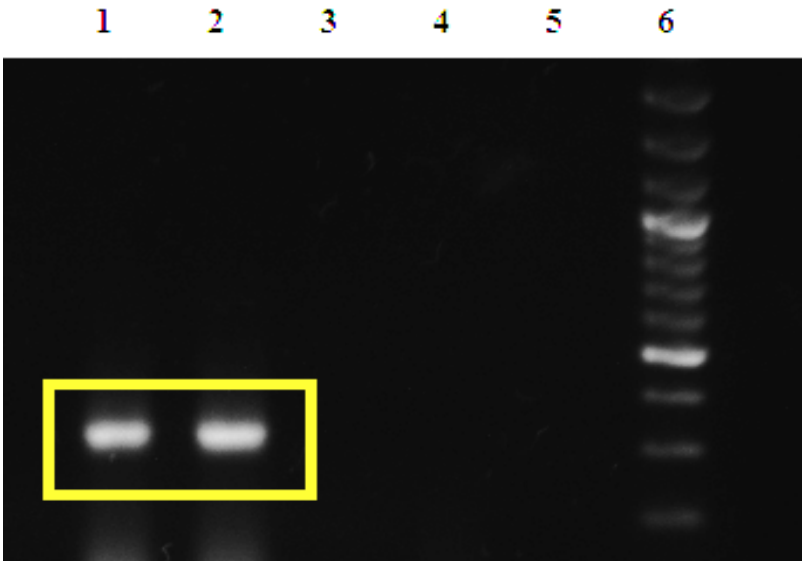

Figure 3.1.2.15. Plasmids were controlled with PCR for the presence of EGFP and mCherry at 1372th position of NR2B. 1. NR2B 1372 EGFP- 1, 2. NR2B 1372 EGFP- 2, 3. NR2B 1372 EGFP- 3, 4. NR2B 1372 EGFP- 4, 5. NR2B 1372 mCherry- 1, 6. DNA ladder. First two plasmids were shown to have EGFP gene.

Figure 3.1.2.16. Plasmids were controlled with PCR for the presence of mCherry at 1372th position of NR2B. Presence of mCherry gene was determined in both plasmids.

CCCTGGACTTCATCCGACGGGAGTCATCCGTCTATGACATCTCAGAGCACCGCCGCAGCTTCACGCATT
CTGACTGCAAATCCTACAACAACCCGCCCTGTGAGGAGAACCTCTTCAGTGACTACATCAGTGAGGTAG
AGAGAACGTTCGGGAACATGGTGAGCAAGGGCGAGGAGCTGTTCACCGGGGTGGTGCCCATCCTGGTCG
AGCTGGACGGCGACGTAAACGGCCACAAGTTCAGCGTGTCCGGCGAGGGCGAGGGCGATGCCACCTACG
GCAAGCTGACCCTGAAGTTCATCTGCACCACCGGCAAGCTGCCCGTGCCCTGGCCCACCCTCGTGACCA
CCCTGACCTACGGCGTGCAGTGCTTCAGCCGCTACCCCGACCACATGAAGCAGCACGACTTCTTCAAGT
CCGCCATGCCCGAAGGCTACGTCCAGG

Figure 3.1.2.17. Presence of EGFP at the right place and frame was confirmed by sequencing.Black bases represent the bases before 972th aminoacid of NR2B and green bases represent EGFP.

CCCTGGACTTCATCCGACGGGAGTCATCCGTCTATGACATCTCAGAGCACCGCCGCAGCTTCACGCATT
CTGACTGCAAATCCTACAACAACCCGCCCTGTGAGGAGAACCTCTTCAGTGACTACATCAGTGAGGTAG
AGAGAACGTTCGGGAACATGGTGAGCAAGGGCGAGGAGGATAACATGGCCATCATCAAGGAGTTCATGC
GCTTCAAGGTGCACATGGAGGGCTCCGTGAACGGCCACGAGTTCGAGATCGAGGGCGAGGGCGAGGGCC
GCCCCTACGAGGGCACCCAGACCGCCAAGCTGAAGGTGACCAAGGGTGGCCCCCTGCCCTTCGCCTGGG
ACATCCTGTCCCCTCAGTTCATGTACGGCTCCAAGGCCTACGTGAAGCACCCCGCCGACATCCCCGACT
ACTTGAAGCTGTCCTTCCCCGAGGGCTTCAAGTGGGAGCGCGTGATGAACTTCGAGGACGGCGGCGTGG
TGACCGTGACCCAGGACTCCTCCCTGCAGGACGGCGAGTTCATCTACAAGGTGAAGCTGCGCGGCAC

Figure 3.1.2.18. Presence of mCherry at the right place and frame was confirmed by sequencing. Black bases represent the bases before 972th aminoacid of NR2B and red bases represent mCherry.

AGCACTCCTACGACACCTTCGTGGACCTGCAGAAGGAAGAAGCCGCCCTGGCCCCGCGCAGCGTAAGCC
TGAAAGACAAGGGCCGATTCATGGATGGGAGCCCCTACGCCCACATGTTTGAGATGTCAGCTGGCGAGA
GCACCTTTGCCAACAACAAGTCCTCAGTGCCCACTGCCGGACATCACCACCACAACAACCCCGGCGGCG
GGTACATGATGGTGAGCAAGGGCGAGGAGCTGTTCACCGGGGTGGTGCCCATCCTGGTCGAGCTGGACG
GCGACGTAAACGGCCACAAGTTCAGCGTGTCCGGCGAGGGCGAGGGCGATGCCACCTACGGCAAGCTGA
CCCTGAAGTTCATCTGCACCACCGGCAAGCTGCCCGTGCCCTGGCCCACCCTCGTGACCACCCTGACCT
ACGGCGTGCAGTGCTTCAGCCGCTACCCCGACCACATGAAGCAGCACGACTTCTTCAAGTCCGCCATGC
CCGAAGGCTACGTCCAGG

Figure 3.1.2.19. Presence of EGFP at the right place and frame was confirmed by sequencing. Black bases represent the bases before 1372th aminoacid of NR2B and green bases represent EGFP.

AGCACTCCTACGACACCTTCGTGGACCTGCAGAAGGAAGAAGCCGCCCTGGCCCCGCGCAGCGTAAGCC
TGAAAGACAAGGGCCGATTCATGGATGGGAGCCCCTACGCCCACATGTTTGAGATGTCAGCTGGCGAGA
GCACCTTTGCCAACAACAAGTCCTCAGTGCCCACTGCCGGACATCACCACCACAACAACCCCGGCGGCG
GGTACATGATGGTGAGCAAGGGCGAGGAGGATAACATGGCCATCATCAAGGAGTTCATGCGCTTCAAGG
TGCACATGGAGGGCTCCGTGAACGGCCACGAGTTCGAGATCGAGGGCGAGGGCGAGGGCCGCCCCTACG
AGGGCACCCAGACCGCCAAGCTGAAGGTGACCAAGGGTGGCCCCCTGCCCTTCGCCTGGGACATCCTGT
CCCCTCAGTTCATGTACGGCTCCAAGGCCTACGTGAAGCACCCCGCCGACATCCCCGACTACTTGAAGC
TGTCCTTCCCCGAGGGCTTCAAGTGGGAGCGCGTGATGAACTTCGAGGACGGCGGCGTGGTGACCGTGA
CCCAGGACTCCTCCCTGCAGGACGGCGAGTTCATCTACAAGGTGAAGCTGCGCGGCAC

Figure 3. 1. 2. 20. Presence of mCherry at the right place and frame was confirmed by sequencing. Black bases represent the bases before 1372th aminoacid of NR2B and red bases represent mCherry.

After confirming the presence of fluorescent proteins at the right place, EGFP labeled constructs were cotransfected to N2a cells with wild type NR1. Figure 3.1.2.21 shows confocal image of EGFP labeled NR2B subunit from 1372th position. This result shows that this strategy did not improve membrane localization of NR2B.

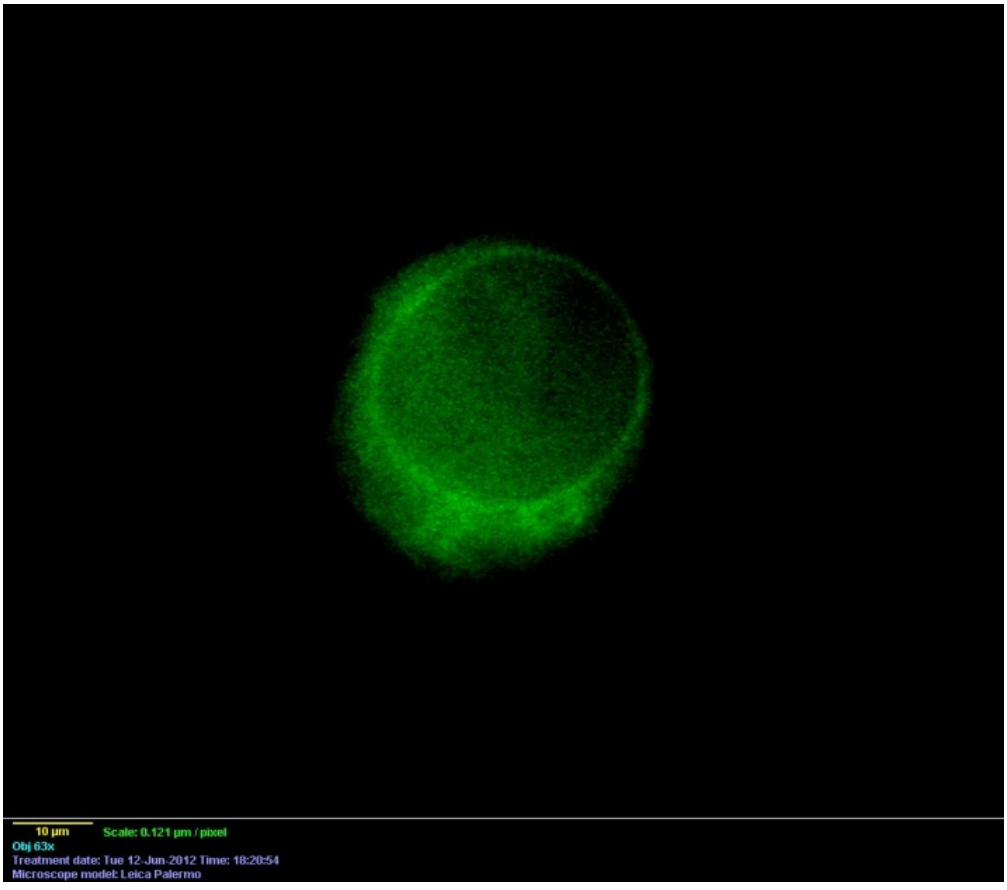

Figure 3.1. 2. 21. Confocal microscope image of EGFP labelled NMDA NR2B subunit from 1372th position when it was cotransfected with NR1 subunit to N2a cells (63x oil objective). This image shows that the distribution of NMDAR was not improved when NR2B subunit was tagged from 1372th position.

Figure 3. 1. 2. 22. Fluorescence microscope image of EGFP labelled NMDA NR2B subunit from 972th position when cotransfected with wild type NR1 subunit to N2a cells. (100 x oil objective). When NR2B subunit was tagged from 972th amino acid, an increased tendency to localize at the membrane was observed.

As indicated by the red arrow in Figure 3.1.2.22, EGFP labeled NR2B subunit from 972th amino acid is found more on the cell projections which may show that labeling from this position allows the interaction with proteins that have role in trafficking of the receptor.
When EGFP label was moved to distal end of C-terminus and cotransfected to N2a cells with wild type NR1, same results were seen as EGFP labeled NR2B from 1372th position (Figure 3.1.2.23).

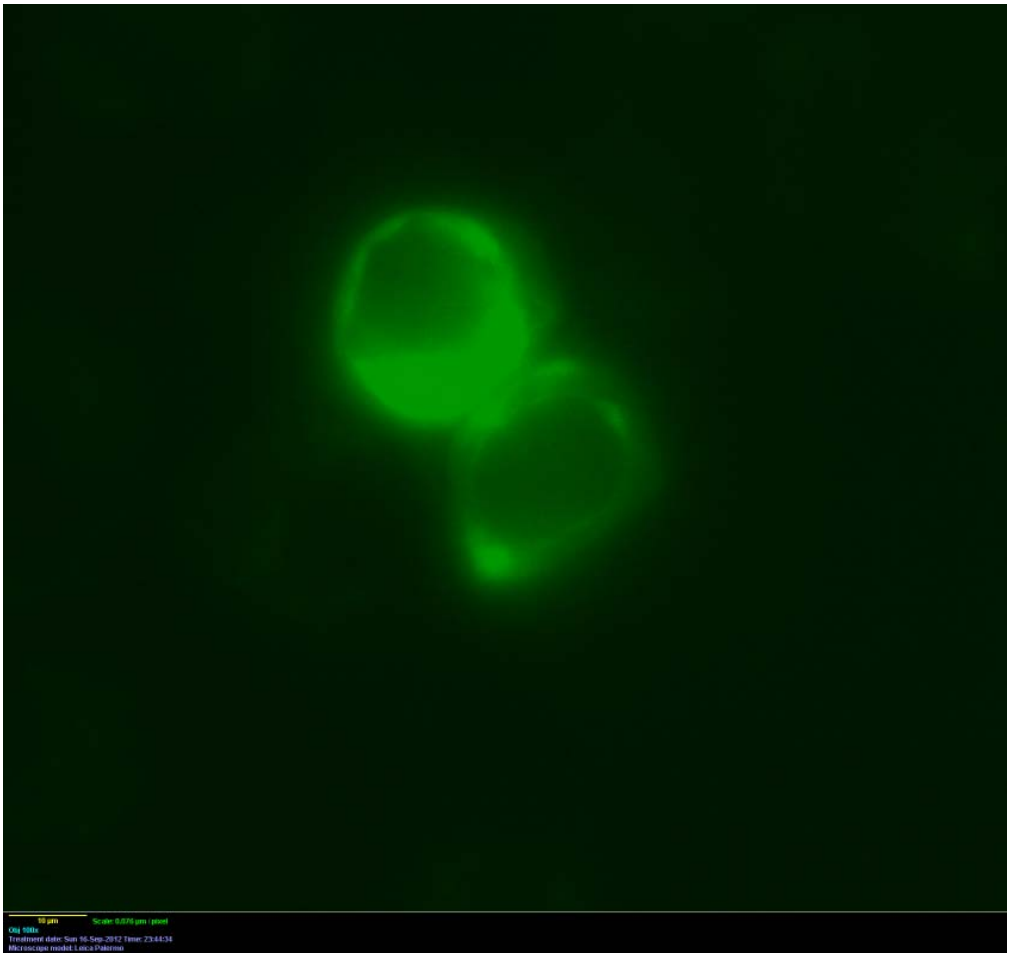

Figure 3. 1. 2. 23. Fluorescence microscope image of EGFP labelled NMDA NR2B subunit from distal end of C-terminus. Construct was cotransfected to N2a cells with wild type NR1 subunit. In this position cell projections disappeared which may suggest that membrane localization which was increased by tagging NR2B subunit from 972th position, decreased by tagging from distal end of C-terminus and from 1372th position.

Moreover we used truncated NR1 which has only N terminal domain (NTD) of the subunit to assess the effect of NR1- NTD on localization and cellular distribution of NR2B. Surprisingly when NR2B was transfected to N2a cells alone no NR2B signal could be detected however when it was cotransfected with NTD of NR1 subunit, NR2B signal intensity and localization was comparable to the signal of NR2B which was cotransfected with full length wild type NR1(Figure3.1.2.24).

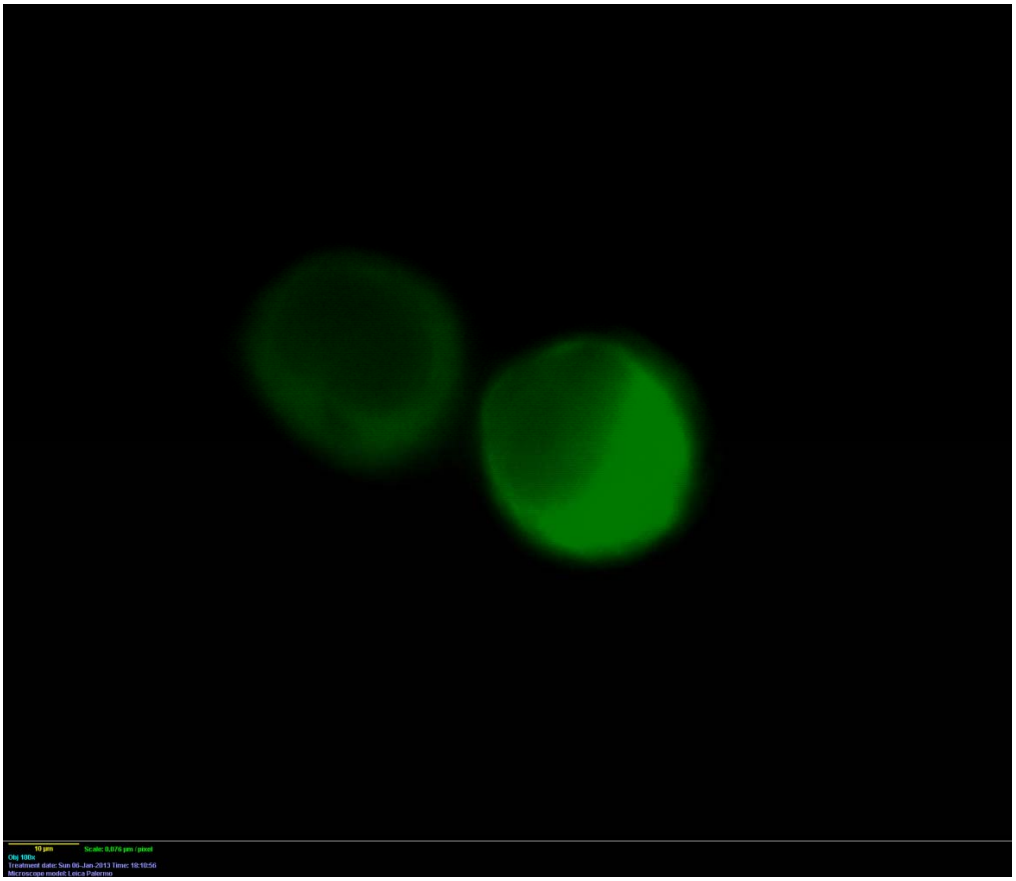

Figure 3. 1. 2. 24. Fluorescent microscope image of NR2B subunit tagged with EGFP from its distal end of C-terminus(100 x oil objective). Tagged subunit was cotransfected with truncated NR1 subunit. Truncated NR1 only have N- terminus. This result may imply that cotransfection of NR2B and NTD of NR1 subunit causes retention of NR2B signal in the cell when compared to its transfection without its counter subunit.

Results indicate that position of the tag change the expression levels of these tagged receptors but not change the localization significantly. Thus, possibility of trafficking problem due to the location of the florescent tags used in this study was ruled out.
In addition, NR2B signal was detected when it was cotransfected with both full length and truncated NR1. However we can not see any signal when NR2B is transfected without NR1. This result points that N terminus of NR1 is ciritical for the survival of NR2B subunit.

3.1.3. DETECTION OF WILD TYPE NMDAR LOCALIZATION IN N2A MOUSE NEUROBLASTOMA CELLS BY IMMUNOCYTOCHEMISTRY

In order to detect what we expect to see by transfecting labeled NMDAR to N2a cell line, wild type N2a NMDARs were labeled with immunocytochemistry. In this study NR1 and NR2B primary antibodies which are able to bind both mouse and human NR1 and NR2B subunits were used. Secondary antibody is raised in donkey for rabbit and conjugated to DyLight 590 for detection.
Immunocytochemistry results show that our fluorescently tagged receptors show a similar distribution pattern with wild type mouse NR1 (Figure 3. 1. 3. 1) and NR2B (Figure 3. 1. 3. 2).

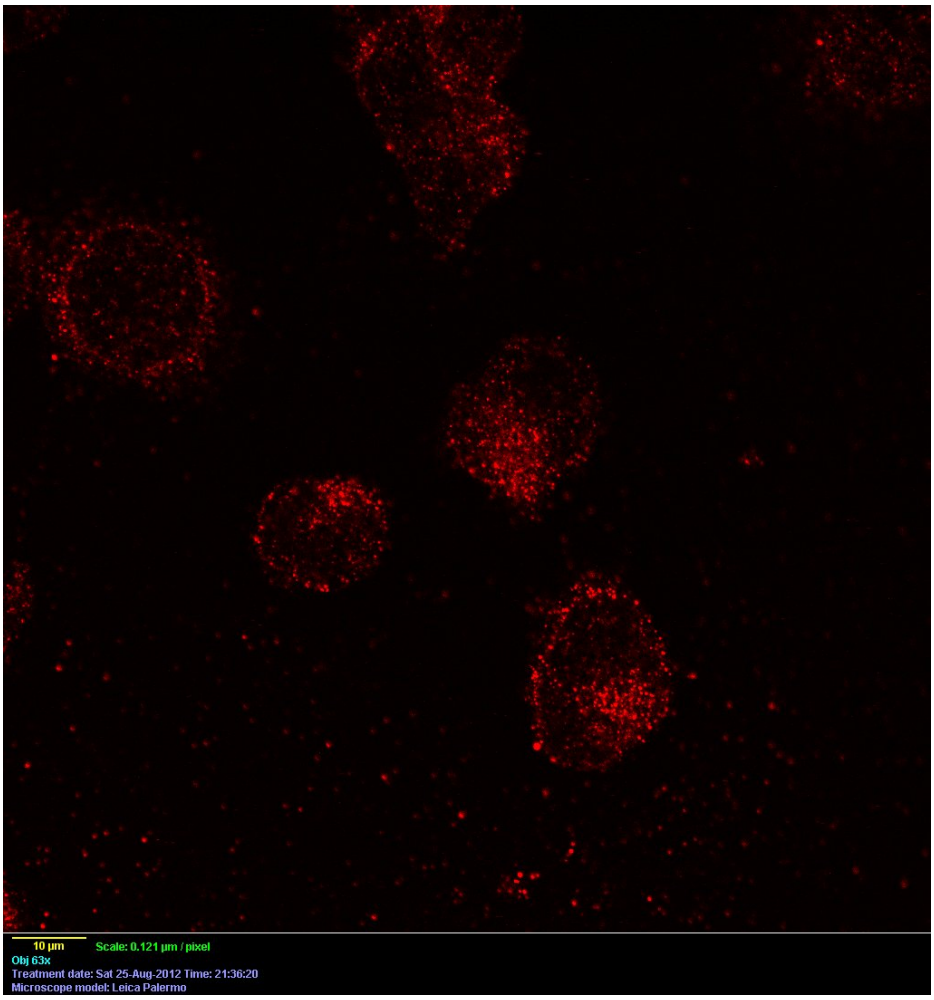

Figure 3. 1. 3. 1. Localization of wild type mouse NR1 subunits in N2a cells were detected by immunocytochemistry. Cells were imaged with confocal microscope (63X oil objective). Primary antibody is against C-terminal tail of NR1 subunit, secondary antibody is labelled with DyLight 590. This image confirms our fluorescent labeling results by showing cytosolic distribution of wild type NR1s in untransfected N2a cells.

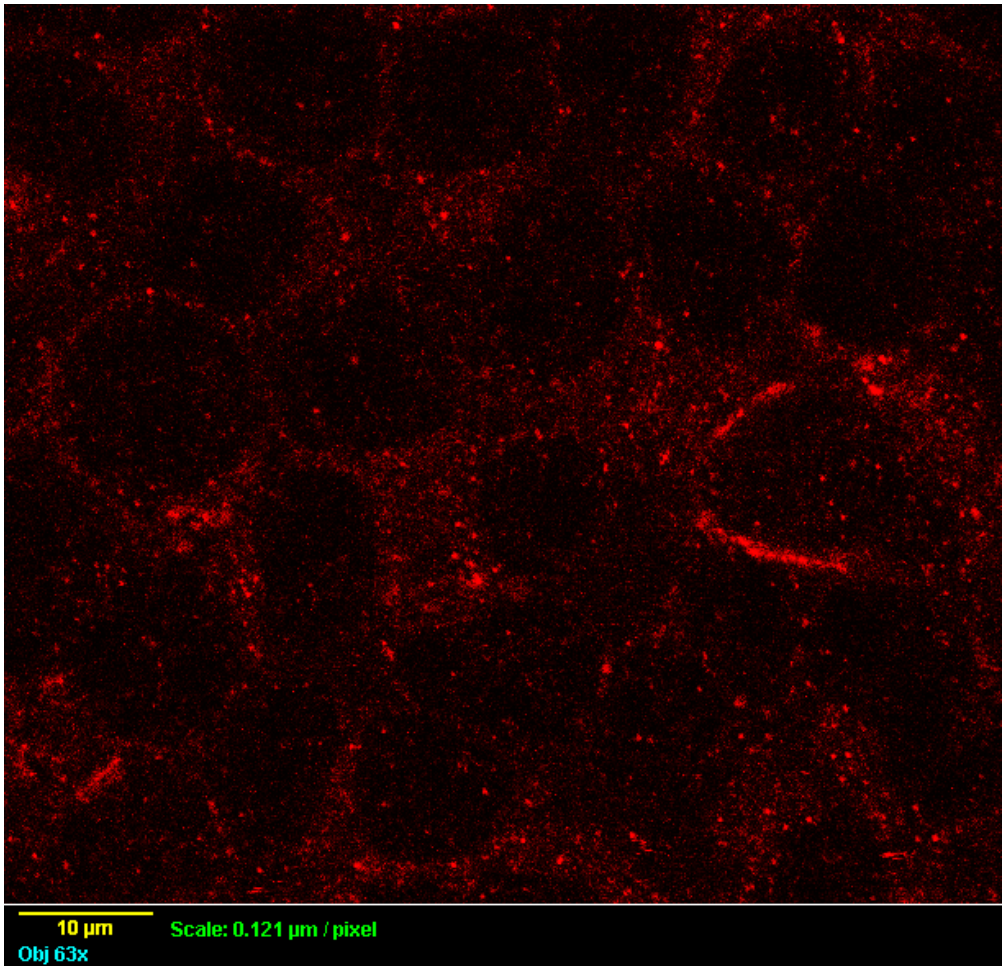

Figure 3. 1. 3. 2. Localization of wild type mouse NR2B was detected by immunocytochemistry. Cells were imaged with confocal microscope (63X oil objective). Primary antibody is against C-terminal tail of NR1 subunit, secondary antibody is labelled with DyLight 590. This image confirms our fluorescent labeling results by showing cytosolic distribution of wild type NR2Bs in untransfected N2a cells.

In order to detect autofluorescence of the cells and the signal coming from unwashed secondary antibody was detected by only applying secondary antibody without primary antibody (Figure 3. 1. 3. 3).

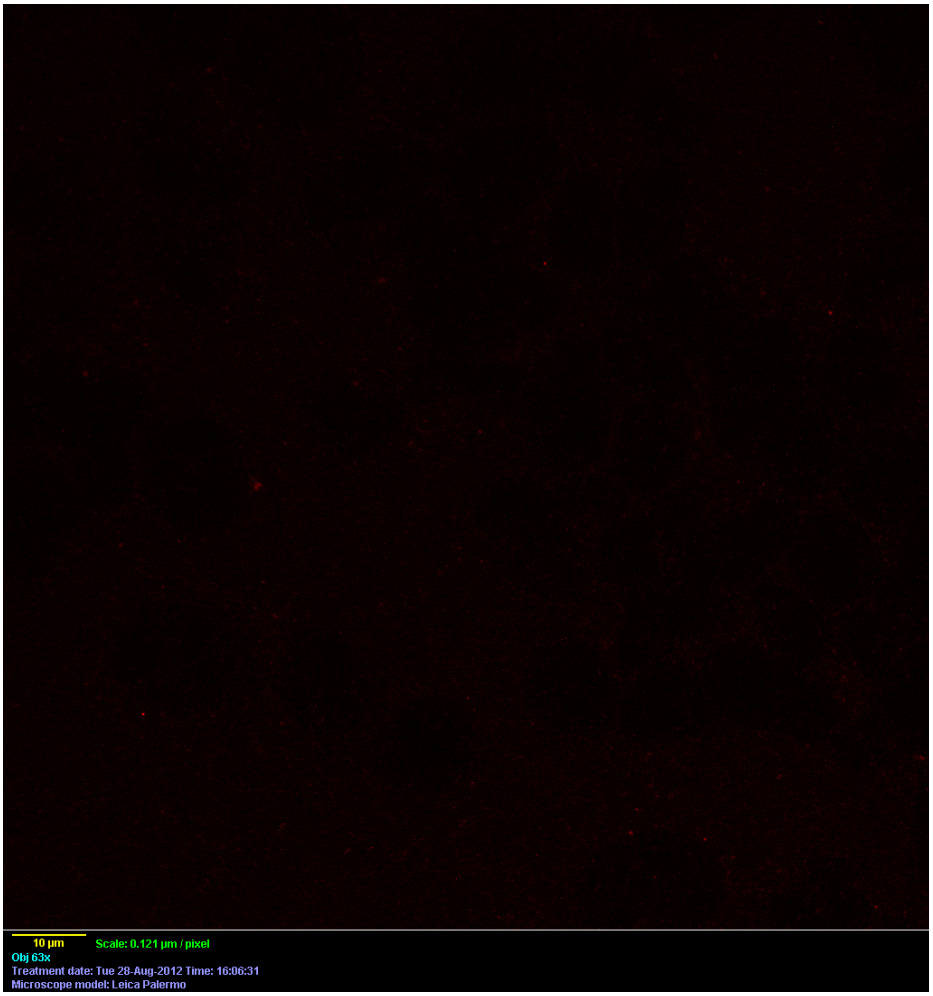

Figure 3. 1. 3. 3. Negative control to detect the signal coming from only secondary antibody. Untransfected N2a cells were treated by all steps of a normal immunocytochemistry procedure except primary antibody addition. With this, nonspecific signal caused by inefficient washing of secondary antibody was detected. Thus, we ensured that NR1 and NR2B signal shown in Figure 3. 1. 3. 1 and Figure 3. 1. 3. 2 are not nonspecific.

3.2. DISCUSSION

In this study, firstly we showed that when fluorescently labelled NR1 subunit is transfected to N2a cells without its counter subunits, unexpectedly NR1 subunit does not reside in the ER. Instead, it exits from the ER and have a more cytosolic distribution pattern. This result can be interpreted in three ways. The first possibility is that, ER retention signal found in the C - tail of NR1 subunit may be masked due to the fluorescent protein that we added to C - tail of NR1 subunit. Although it seems possible, presence of cytosolic signal after moving fluorescent protein tag weakens this hypothesis. Secondly, wild type NMDAR subunits that are naturally

found in N2a cells may be assembled with labelled NR1 subunits. However if the overexpression of labelled NR1 is considered, availability of counter subunits in this level seems to have slight probability. Even if it is, we should have seen signal when NR2B subunit is transfected without NR1 subunit. Lastly, NR1 subunit may not reside in the ER in natural state. Although it conflicts with the literature, this hypothesis can be supported with further experiments by tagging NR1 subunit from its N terminus and transfecting it to NMDAR knock out neuronal cell line since trafficking proteins are absent in nonneuronal cell lines.

We also showed that when labelled NR2B subunit is transfected without its counter subunit NR1, any signal was not detected. This result suggest that, either labelled NR2Bs assembled with wild type NR1s are too low to detect or NR2B subunit is prematurely degraded due to unassembly of the subunit. To be sure about premature degradation hypothesis, level of NR2B subunit can be detected by using western blot in a cell line that does not have wild type NMDARs. After having negative results in the transfection of labelled NR2B subunit without NR1, labelled NR2B and truncated NR1 which has only N terminal domain were cotransfected to N2a cells and NR2B signal was detected. Based on this result we speculate that assembly of NR2B subunit with N terminal domain of NR1 subunit prevents premature degradation of NR2B. Assuming it is so, degradation of NR2B subunit may be regulated by its N terminus.

Moreover, localization of assembled NMDAR was also unexpectedly different from the literature which was not supported with consistent microscope images. In theory, assembled NMDAR trafficked from ER to the membrane by forming an exocyst complex on C tail of NMDAR subunits. To be able to support this information by fluorescence microscopy NR1 subunit was tagged with mCherry and EGFP fluorescent proteins from their distal end of C-terminus. However when tagged NR1 was cotransfected with wild type NR2B, it was seen that NR1 subunits were cytosolic. Since PDZ domain is involved in the trafficking of NMDARs to the membrane, an extra PDZ domain was added to the end of tagged NR1 subunit to rule out the possibility that we could mask PDZ domain with fluorescent proteins and affect its trafficking. However even after addition of extra PDZ domain, cytosolic distribution pattern of NMDAR persisted. So we concluded that extra PDZ domain did not help delivery of the receptor to the membrane. Then in order to rule out the possibility of masking of critical modification sites so affecting trafficking of NMDAR to the membrane, fluorescent proteins were moved to an internal site. While deciding on this site, not only experimental but also hypothetical modification sites by similarity were assessed and the position that is furthest from any modification site was selected as labelling point. However distribution pattern of NR1 did not change with this strategy. Similarly NMDAR signal coming from NR1 subunit was cytosolic. Then by considering the possibility of getting signal from intacellular pool of NR1, NR2B was tagged with EGFP and mCherry from its distal end of C-terminus, 972^{th} amino acid and 1372^{th} amino acid. 972^{th} and 1372^{th} positions were selected by using the same strategy as NR1. Since NR2B does not give signal when it is transfected alone, any signal coming from NR2B would show us the NMDARs. When these NR2B constructs were transfected with wild type NR1 subunit, it was supported that assembled NMDARs do not show a localized pattern on the membrane.

Furthermore in order to detect the distribution pattern of wild type NMDARs in untransfected N2a cells, NR1 and NR2B subunits were labelled with immunocytochemistry. Results of immunocytochemistry on untransfected N2a cell line confirm the cytosolic pattern of NR1/NR2B subunits and NMDAR. Thus this result shows that tagging of NMDAR subunits with fluorescent proteins does not effect localization of NMDA receptors. Due to cross reactivity of NR1 and NR2B antibodies between mouse and human receptors, we could not observe localization of wild type human NMDARs in N2a cells.

To sum up; in this study, primarily we showed that on the contrary to literature, NMDARs does not have an isolated trafficking on the vesicles and compartments. Instead it has a cytosolic pattern before its delivery to the membrane where shows its acitivity. In addition, altough it needs to be supported with additional data such as western blot on NMDAR knock out neuronal cell lines, our study show an approach to premature degradation of unassembled

NR2B subunit. Furthermore the effect of fluorescent protein labelling on the distribution pattern of NMDARs was assessed for the first time. With further studies assessing the effect of fluorescent protein labelling on the activity of NMDARs, the constructs prepared in this study can be used for many applications such as trafficking and interaction studies of NMDARs.
Ultimately, an *in vitro* system based on fluorescent protein tagging of NMDARs for modelling of a variety of NMDAR mediated disorders can be constructed by using this approach. This system can be used to reveal mechanisms of disorders, localization, trafficking and interaction changes due to these disorders such as schizophrenia, Parkinson's disease and Alzheimer's disease. Furthermore, this system can be used for efficient cell culture based testing and monitoring of effects of antipsychotic drugs targeting the mechanisms in which NMDARs are involved.

REFERENCES

Aidley, D. J., Stanfield, P. R. (1996). Ion Channels:Molecules in Action. Cambridge: Cambridge University Press. 1-8.

Atlason, P. T., Garside, M. L, Meddows, E., Whiting, P., McIlhinney. R. A. J. (2007). N-Methyl-D-aspartate (NMDA) receptor subunit NR1 forms the substrate for oligomeric assembly of the NMDA receptor. J Biol Chem, 282, 25299-25307.

Beaulieu, J. M., Gainetdinov, R. R. (2011). The Physiology, Signaling, and Pharmacology of Dopamine Receptors. Pharmacological Reviews. 63 , 182-217.

Bouvier, M. (2001). Oligomerization of G-protein-coupled transmitter receptors.Nature Reviews Neuroscience. 2, 274-286

Carroll, R. C., Zukin, R. S. (2002). NMDA-receptor trafficking and targeting: implications for synaptic transmission and plasticity. TRENDS in Neuroscience. 25 (11), 571-577.

Clegg, R. M. (1996). Fluorescence resonance energy transfer. In Fluorescence Imaging Spectroscopy and Microscopy (Wang, X.F. and Herman, B., eds), pp. 179–252, John Wiley & Sons.

Corry, B. (2006). Understanding ion channel selectivity and gating and their role in cellular signalling.Molecular BioSystems, 2. 527-535.

Cull-Candy, S., Brickley, S., Farrant, M. (2001). NMDA receptor subunits: diversity, development and disease. Current Opinion in Neurobiology, 11, 327-335.

Dascal, N. (2001). Ion Channel Regulation by G Proteins. TRENDS in Endocrinology & Metabolism, 12(9), 391-398.

Doherty, A., Coutinho, V., Collingridge, G. and Henley J. (1999). Rapid internalization and surface expression of a functional, fluorescently tagged G-protein-coupled glutamate receptor. Biochem. J., 341 ,415–422

Dravid, S. M., Prakash, A., Traynelis, S. F. (2008) Activation of recombinant NR1/NR2C NMDA receptors. J Physiol, 586, 4425-39.

du Bois, T. M., et al. (2008). Altered dopamine receptor and dopamine transporter binding and tyrosine hydroxylase mRNA expression following perinatal NMDA receptor blockade. Neurochem. Res., 33, 1224–1231.

Ewald, R. C., Cline, H. T. NMDA Receptors and Brain Development. In: Van Dongen AM, editor. Biology of the NMDA Receptor. Boca Raton (FL): CRC Press; 2009. Chapter 1. Available from: http://www.ncbi.nlm.nih.gov/books/NBK5287/

Farina, A. N., Blain, K. Y., Maruo, T., Kwiatkowski, W., Choe, S., Nakagawa, T. (2011). Separation of Domain Contacts Is Required for Heterotetrameric Assembly of Functional NMDA Receptors. The Journal of Neuroscience. 31 (10), 3565-3579.

Ferguson, S. S. (2001). Evolving concepts in G protein-coupled receptor endocytosis: the role in receptor desensitization and signaling. Pharmacol Rev, 53, 1–24.

Ferguson, S. S., Barak, L. S., Zhang, J., Caron, M. G. (1996) G-protein-coupled receptor regulation: role of G-protein-coupled receptor kinases and arrestins. Can J Physiol Pharmacol, 74, 1095–1110.

Fredriksson, R., Lagerstrom, M. C., Lundin, L. G., Schioth, H. B. (2003) . The G-protein-coupled receptors in the human genome form five main families. Phylogenetic analysis, paralogon groups, and fingerprints,Mol. Pharmacol, 63 (6), 1256–1272.

Förster, T. (1948). Intermolecular Energy Migration and Fluorescence Ann. Phys, 2, 55-75.

Furukawa, H., Singh, S. K., Mancusso, R., Gouaux, E. (2005). Subunit arrangement and function in NMDA receptors. Nature, 438 , 185-192.

Gabashvili, I. S., Sokolowski, B. H., Morton, C. C., Giersch, A. B. (2007). Ion channel gene expression in the inner ear. J. Assoc. Res. Otolaryngol, 8, 305–328.

Gainetdinov, R. R., Premont, R. T., Bohn, L. M., Lefkowitz, R. J., Caron, M. G. (2004). Desensitization of G protein-coupled receptors and neuronal functions. Annu Rev Neurosci 27, 107–144.

Guillaud, L., Setou, M., Hirokawa, N. (2003). KIF17 dynamics and regulation of NR2B trafficking in hippocampal neurons. J Neurosci, 23,131-140.

Hansen, H. H., Briem, T., Dzietko, M. (2004). Mechanisms leading to disseminated apoptosis following NMDA receptor blockade in the developing rat brain. Neurobiol Dis, 16, 440–453.

Harmar, A. J., Hills, R. A., Rosser, E. M. (2009). IUPHAR-DB:the IUPHAR database of G protein-coupled receptors and ion channels. Nucl. Acids Res. 37 (Database issue): D680-D685. Retrieved June 21, 2012, from: http://www.iuphar-db.org/DATABASE/ReceptorFamilies Forward?type=IC

Hawkins, L. M., Prybylowski, K., Chang, K., Moussan, C., Stephenson, F. A., Wenthold, R. J. (2004). Export from the endoplasmic reticulum of assembled NMDA receptors is controlled by a motif in the C-terminus of the NR2 subunit.J Biol Chem, 279, 28903-28910.

Hazelwood, L. A., Free, R. B., Sibley, D. R. (2009). Dopamine Receptor-Interacting Proteins. In: Neve,KA The Dopamine Receptors. 2nd ed. New York: Humana Press. 219-254.

Hippe, A., Bylaite, M., Chen M., von Mikecz, A., Wolf, R., Ruzicka, T., Walz, M. (2006). Expression and tissue distribution of mouse *Hax1*. Gene, 379, 116-126.

Hollmann, M. and Heinemann, S. (1994). Cloned Glutamate Receptors.Annual Review of Neuroscience, 17, 31-108.

Huettner, J. E. (2003). Kainate receptors and synaptic transmission. Prog. Neurobiol. 70 (5), 387–407.

Huh, K. H., Wenthold, R. J. (1999). Turnover analysis of glutamate receptors identifies a rapidly degraded pool of the N-methyl-D-aspartate receptor subunit, NR1, in cultured cerebellar granule cells. J Biol Chem, 274(1), 151–7.

Ikonomidou, C., Bosch, F., Miksa, M. (1999). Blockade of NMDA receptors and apoptotic neurodegeneration in the developing brain. Science, 283, 70–74

Kim, E., Sheng, M. (2004). PDZ domain proteins of synapses.Nature Rev Neurosci, 5, 771-781.

Kobilka, B. K. (2007). G protein coupled receptor structure and activation.Biochimica et Biophysica Acta, 1768 ,794–807.

Köhr, G. (2006). NMDA receptor function: subunit composition versus spatial distribution. Cell Tissue Research., 326 , 439-446.

Krystal, J. H., Karper, L. P., Seibyl, J. P., Freeman, G. K., Delaney, R., Bremner, J. D., Heninger, G. R., Bowers, M. B., Charney, D. S. (1994). Subanesthetic effects of the noncompetitive NMDA antagonist, ketamine, in humans: psychotomimetic, perceptual, cognitive, and neuroendocrine responses. Arch Gen Psychiatry, 51, 199–214.

Laurie, D. J., Seeburg, P. H. (1994). Regional and Developmental Heterogeneity in Splicing of the Rat Brain NMDAR 1 mRNA. The Journal of Neuroscience, 14 (5), 3180-3194.

Law, A. J., Weickert, C. S., Webster, M. J., Herman, M. M., Kleinman, J.E. (2003) Expression of NMDA receptor NR1, NR2A and NR2B subunit mRNAs during development of the human hippocampal formation. Eur J Neurosci, 18, 1197–1205.

Lee, C. H., Gouaux, E. (2011). Amino Terminal Domains of the NMDA Receptor Are Organized as Local Heterodimers. Public Library of Science, 6 (4), e19180.

Lee, F. J., Xue, S., Pei, L., et al. (2002). Dual regulation of NMDA receptor functions by direct proteinprotein interactions with the dopamine D1 receptor. Cell, 111(2), 219–30.

Liu, L., Wong, T. P., Pozza, M. F., Lingenhoehl, K., Wang, Y., Sheng, M., Auberson, Y. P., Wang, Y. T. (2004). Role of NMDA Receptor Subtypes in Governing the Direction of Hippocampal Synaptic Plasticity . Science, 304 , 1021-1024.

Liu, X. Y., Chu, X. P., Mao, L. M., Wang, M., Lan, H. X., Li, M. H., Zhang, G. C., Parelkar, N. K., Fibuch, E. E., Haines, M., Neve, K. A., Liu, F., Xiong, Z. G., Wang, J. Q. (2006). Modulation of D2R-NR2B interactions in response to cocaine. Neuron, 52, 897-909

Lohse, M. J., Benovic, J. L., Codina, J., Caron, M. G., Lefkowitz, R. J. (1990). beta-Arrestin: a protein that regulates beta-adrenergic receptor function. Science, 248, 1547–1550

Lu, Y. M., Roder, J. C., Davidow, J., Salter, M. W. (1998). Src Activation in the Induction of Long-Term Potentiation in CA1 Hippocampal Neurons.Science, 279, 1363-1368.

Meddows, E., Bourdelles, B. L., Grimwood, S., Wafford, K., Sandhu, S., Whiting, P., McIlhinney, R. A. J. (2001). Identification of Molecular Determinants That Are Important in the Assembly of N-Methyl-D-aspartate Receptors. The Journal of Biological Chemistry, 276(22), 18795-18803.

Missale, C., Fiorentini, C., Collo, G., Spano, P. (2010). The neurobiology of dopamine receptors: evolution from the dual concept to heterodimer complexes. J.Recept. Signal Transduct. Res., 30, 347–354.

Mohn, A. R., Gainetdinov, R. R., Caron, M. G., Koller, B. H. (1999) Mice with reduced NMDA receptor expression display behaviors related to schizophrenia. Cell , 98, 427–436.

Moreira, I. S., Shi, L., Freyberg, Z., Ericksen, S. S., Weinstein, H., Javitch, J. A. (2009). Structural Basis of Dopamine Receptor Activation. In: Neve,KA.The Dopamine Receptors. 2nd ed. New York: Humana Press. 47-74.

Mullasseril, P., Hansen, K. B., Vance, K. M., Ogden, K. K., Yuan, H., Kurtkaya, N. L., Santangelo, R., Orr, A. G., Le, P., Vellano, K. M., Liotta, D. C., Traynelis, S. F. (2010). A subunit-selective potentiator of NR2C- and NR2D-containing NMDA receptors. Nat Commun, 1, 90.

Paila, Y. D., Chattopadhyay, A. (2009). The function of G-protein coupled receptors and membrane cholesterol: specific or general interaction?Glycoconj J., 26, 711-720.

Paoletti, P. (2011). Molecular basis of NMDA receptor functional diversity. European Journal of Neuroscience, 33, 1351-1365.

Philpot, B. D., Sekhar, A. K., Shouval, H. Z., Bear, M. F. (2001). Visual experience and deprivation bidirectionally modify the composition and function of NMDA receptors in visual cortex. Neuron, 29(1), 157–69.

Prybylowski, K., Wenthold, R. J. (2004). N-Methyl-D-aspartate Receptors: Subunit Assembly and Trafficking to the Synapse. The Journal of Biological Chemistry, 279 (11), 9673-9676.

Rankin, M. L., Hazelwood, L. A., Free, R. B., Namkung, Y., Rex, E. B., Roof, R. A., Sibley, D. R. (2010). Molecular pharmacology of the dopamine receptors, in Dopamine Handbook (Iversen, L. L., Dunnett, S. B., Iversen, S. D., Bjorklund, A. ed) 63–87, Oxford University Press, New York.

Roche, K. W., Standley, S., McCallum, J., Ly, C. D., Ehlers, M. D., Wenthold, R. J. (2001). Molecular determinants of NMDA receptor internalization.Nat. Neurosci,. 4, 794–802

Rosenbaum, D. M., Rasmussen, S. G. F., Kobilka, B. K. (2009). The structure and function of G-protein-coupled receptors. Nature, 459 (1), 356-363.

Sans, N., Prybylowski, K., Petralia, R. S., Chang, K., Wang, Y. X., Racca, C., Vicini, S., Wenthold, R. J. (2003). NMDA receptor trafficking through an interaction between PDZ proteins and the exocyst complex. Nat Cell Biol, 5, 520-530.

Sans, N., Wang, P. Y., Du, Q., Petralia, R. S., Wang, Y. X., Nakka, S., Blumer, J. B., Macara, I. G., Wenthold, R. J. (2005). mPins modulates PSD-95 and SAP102 trafficking and influences NMDA receptor surface expression.Nat. Cell Biol, 7, 1179-1190.

Sanz-Clemente, A., Nicoll, R. A., Roche, K. W. (2012). Diversity in NMDA Receptor Composition:Many Regulators, Many Consequences.Available:http://nro.sagepub.com/content/early/2012/02/15/1073858411435129. Last accessed 26th April 2012.

Schorge, S., Colquhoun, D. (2003). Studies of NMDA Receptor Function and Stoichiometry with Truncated and Tandem Subunits.Journal of Neuroscience, 23(4), 1151–1158.

Seeman, P. (2009). Dopamine Receptor-Interacting Proteins. In: Neve, K. A. The Dopamine Receptors. 2nd ed. New York: Humana Press.1-22.

Setou, M., Nakagawa, T., Seog, D. H., Hirokawa, N. (2000). Kinesin superfamily motor protein KIF17 and mLin-10 in NMDA receptor-containing vesicle transport. Science, 288, 1796-1802.

Sibley, D. R. (1999). New insights into dopaminergic receptor function using antisense and genetically altered animals. Annu Rev Pharmacol Toxicol, 39, 313–341.

Soderling, T. R., Derkach, V. A. (2000). Postsynaptic protein phosphorylation and LTP. Trends in Neurosciences, 23 (2), 75-80.

Stephenson, F. A., Cousins, S. L., Kenny, A. V. (2008). Assembly and forward trafficking of NMDA receptors. Molecular Membrane Biology, 25 (4), 311-320.

Tabassum, N., Feroz, A. (2011). Ion Channels and their Modulation. Journal of Applied Pharmaceutical Science, 01(1), 20-25.

Thastrup, O., Tullin, S., Kongsbak Poulsen, L., Bjørn, S. (2001)."Fluorescent Proteins". US patent.

Tramier, M., Zahid, M., Mevel, J. C., Masse, M. J., Coppey-Moisan, M. (2006). Sensitivity of CFP/YFP and GFP/mCherry pairs to donor photobleaching on FRET determination by fluorescence lifetime imaging microscopy in living cells. Microscopy Research and Technique, 69, 933-939.

Traynelis, S.F., Hartley, M., Heinemann,S.F. (1995). Control of proton sensitivity of the NMDA receptor by RNA splicing and polyamines. Science, 268, 873-876.

Umbricht, D., Schmid, L., Koller, R., Vollenweider, F. X., Hell, D., Javitt, D. C. (2000). Ketamine-induced deficits in auditory and visual context-dependent processing in healthy volunteers: Implications for models of cognitive deficits in schizophrenia. Arch. Gen. Psychiatry, 57, 1139–1147.

Usiello, A., Baik, J. H., Rouge´-Pont, F., Picetti, R., Dierich, A., LeMeur, M., Piazza, P. V., Borrelli, E. (2000). Distinct functions of the two isoforms of dopamine D2 receptors.Nature, 408, 199–203.

Vandenberghe, W., Robberecht, W., Brorson, J. R. (2000) AMPA receptor calcium permeability, GluR2 expression, and selective motoneuron vulnerability. J Neurosci, 20(1), 123-132.

Vissel, B., Krupp, J. J., Heinemann, S. F.,Westbrook, G. L. (2001). A use-dependent tyrosine dephosphorylation of NMDA receptors is independent of ion flux. Nat. Neurosci, 4, 587–96

Wenthold, R. J., Prybylowski, K., Standley, S., Sans, N., Petralia, R. S. (2003). Trafficking of NMDA Receptors. Annual Reviews Pharmacology an Toxicology, 43, 335-358.

Wreggett, K. A., Seeman, P. (1984). Agonist high- and low-affinity states of the D2 dopamine receptor in calf brain: partial conversion by guanine nucleotide. Mol Pharmacol, 25, 10–17.

Yang,W., Zheng, C., Song, Q., Yang, X., Qiu, S., Liu, C., Chen, Z., Duan, S., Luo, J. (2007). A Three Amino Acid Tail Following the TM4 Region of the N-Methyl-D-aspartate Receptor (NR) 2 Subunits Is Sufficient to Overcome Endoplasmic Reticulum Retention of NR1-1a Subunit. The Journal of Biological Chemistry, 282(12), 9269-9278.

Yashiro, K., Philpot, B. D. (2008). Regulation of NMDA Receptor Subunit Expression and Its Implications for LTD, LTP, and Metaplasticity.Neuropharmacology, 55 (7), 1081-1094

APPENDIX A

NEURO2A CELL CULTURE MEDIUM

Table A.1 Composition of D-MEM with High Glucose

COMPONENT	**CONCENTRATION (mg/L)**
Amino Acids	
Glycine	30
L-Arginine hydrochloride	84
L-Cysteine 2HCl	63
L-Glutamine	580
L-Histidine hydrochloride-H_2O	42
L-Isoleucine	105
L-Leucine	105
L-Lysine hydrochloride	146
L-Methionine	30
L-Phenylalanine	66
L-Serine	42
L-Threonine	95
L-Tryptophan	16
L-Tyrosine	72
L-Valine	94
Vitamins	
Choline chloride	4
D-Calcium pantothenate	4
Folic acid	4
Niacinamide	4
Pyridoxine hydrochloride	4

Table A.1 (cont'd). Composition of D-MEM with High Glucose

Riboflavin	0.4
Thiamine hydrochloride	4
i-Inositol	7.2
Inorganic Salts	
Calcium chloride	264
Ferric nitrate	0.1
Magnesium sulfate	200
Potassium chloride	400
Sodium bicarbonate	3700
Sodium chloride	6400
Sodium phosphate monobasic	141
Other components	
D-Glucose (Dextrose)	4500
Phenol Red	15
Sodium pyruvate	110

Composition of 1X Phosphate Buffered Saline

8g/L NaCl
0.2g/L KCl
1.44g/L Na_2HPO_4
0.24g/L KH_2PO_4

APPENDIX B

BACTERIAL CULTURE MEDIA PREPARATION

Luria- Bertani (LB) Medium

10 g/L tryptone
5 g /Lyeast extract
5 g/L NaCl

15 g/L agar is added to LB for solid agar medium preparation, pH is adjusted to 7.

APPENDIX C

BUFFERS & SOLUTIONS

1X NEBuffer 1:

10 mM Bis-Tris-Propane-HCl
10 mM $MgCl_2$
1 mM Dithiothreitol pH 7.0 at 25°C

1X NEBuffer 2:

10 mM Tris-HCl
50 mM NaCl
10 mM $MgCl_2$
1 mM Dithiothreitol pH 7.9 at 25°C

1X NEBuffer 3:

50 mM Tris-HCl
100 mM NaCl
10 mM $MgCl_2$
1 mM Dithiothreitol pH 7.9 at 25°C

1X NEBuffer 4:

20 mM Tris-acetate
50 mM potassium acetate
10 mM Magnesium Acetate
1 mM Dithiothreitol pH 7.9 at 25°C

1X T4 DNA Ligase Reaction Buffer:

50 mM Tris-HCl
10 mM $MgCl_2$
1 mM ATP
10 mM Dithiothreitol pH 7.5 at 25°C

10X TBE (Tris-Borate-EDTA) Buffer

Component	Amount	Concentration
Tris Base	108 g	890 mM Boric Acid 55 g
890 mM EDTA	40 ml	20 mM

Composition of 6X Loading Dye

10 mM Tris-HCl (pH 7.6)
0.03% bromophenol blue
0.03% xylene cyanol FF
60% glycerol
60 mM EDTA

Preparation of 4% Formaldehyde Solution

40g/L paraformaldehyde is dissolved in 1X PBS at 60^{o}C by adding 1N NaOH.
pH is adjusted to 6.9.
Solution was filter sterilized.

Composition of Immunocytochemistry Wash Buffer

0.1% BSA in 1X PBS

Composition of Immunocytochemistry Blocking Buffer

1% BSA in 1X PBS

Composition of Immunocytochemistry Dilution Buffer

1% BSA
0.3% Triton X-100 in 1X PBS

Transformation Buffer I (Tfb I)

30 mM KOAc
100 mM RbCl2
10 mM RbCl2
50 mM MnCl2
15% Glycerol (v/v)
pH = 5.8

Transformation Buffer II (Tfb II)

10 mM MOPS (or PIPES)
75 mM $CaCl_2$
10 mM $RbCl_2$
15% Glycerol (v/v)
pH = 6.5

APPENDIX D

PLASMID MAPS

pReceiver Vector:

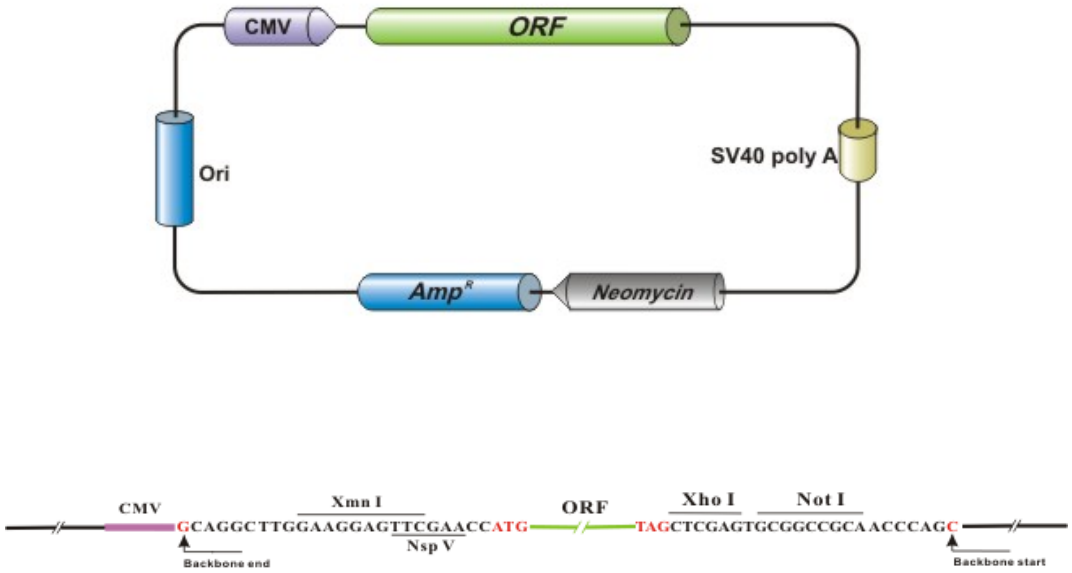

Figure D.1. Map of pReceiver vector

pCR-4-TOPO Vector:

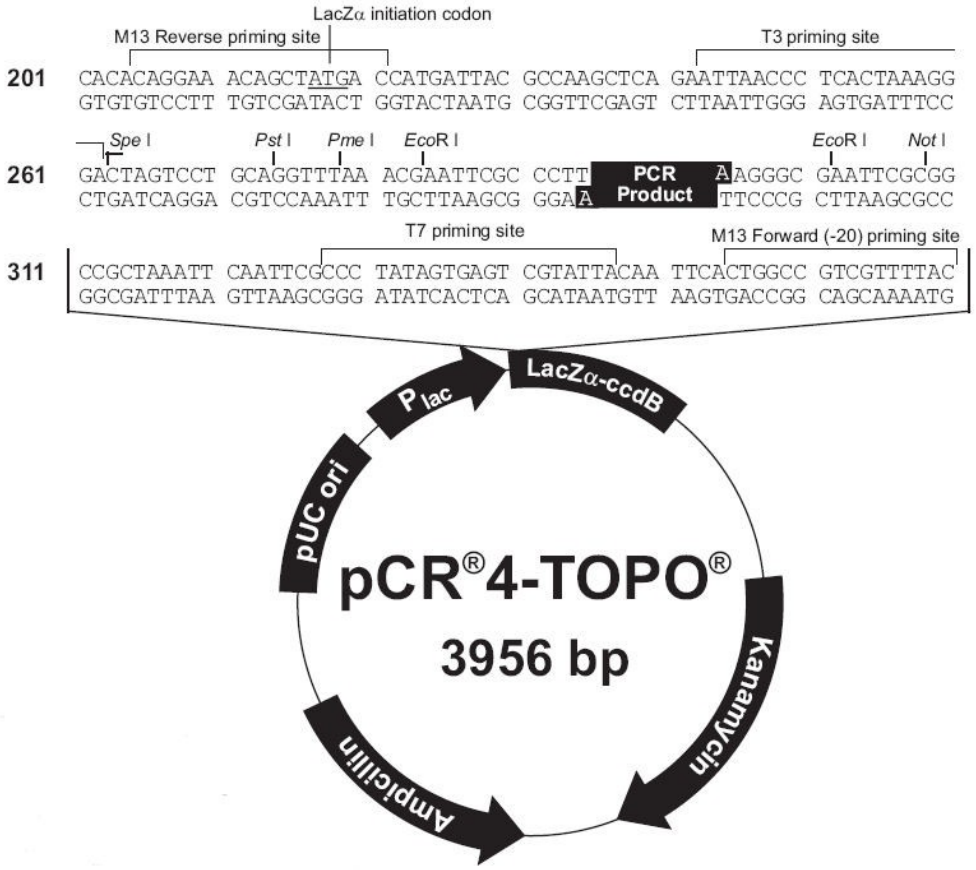

Figure D. 2. Map of pCR 4-TOPO vector

pCR-XL-TOPO:

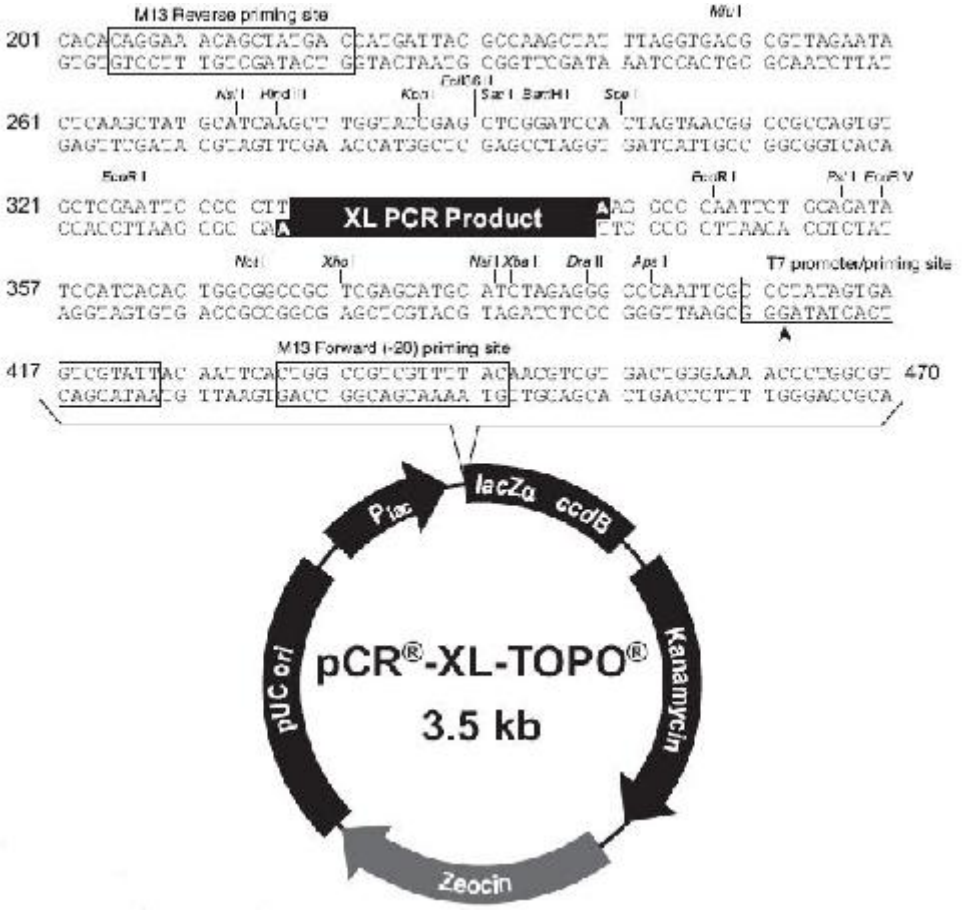

Figure D. 3. Map of pCR-XL TOPO vector

pCDNA 3.1(-) vector:

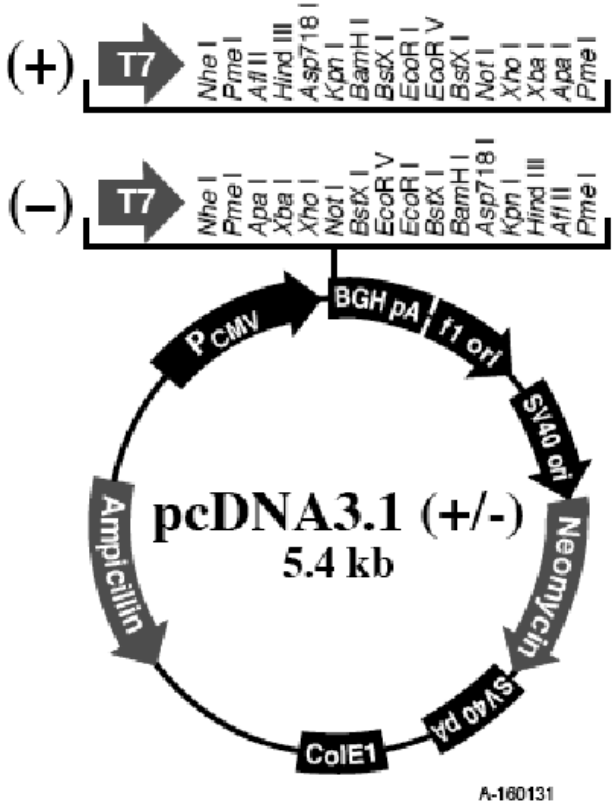

Figure D. 4. Map of pCDNA 3. 1 (-) vector